Preparation of Silica Aerogels with Improved Mechanical Properties and Extremely Low Thermal Conductivities through Modified Sol-Gel Process

by

Yanjia Zuo

B.S. Chemistry
Tsinghua University, P.R. China, 2005

SUBMITTED TO THE DEPARTMENT OF MECHANICAL ENGINEERING IN PARTIAL FULFILLMENT OF THE REQUIREMENTS FOR THE DEGREE OF

MASTER OF SCIENCE IN MECHANICAL ENGINEERING
AT THE
MASSACHUSETTS INSTITUTE OF TECHNOLOGY

JUNE 2010

Signature of Autho 0 1
Department of Mechanical Engineering
May 06, 2010

Certified by:..... .....
Taofang Zeng
Principal Research Scientist, Department of Mechanical Engineering
Thesis Supervisor

Certified by:..... .....
Gang Chen
Carl Richard Soderberg Professor, Department of Mechanical Engineering
Thesis Co-Supervisor

Accepted by:..... .....
David E.Hardt
Chairman, Department Committee for Graduate Students

Preparation of Silica Aerogels with Improved Mechanical Properties and Extremely Low Thermal Conductivities through Modified Sol-Gel Process

by

Yanjia Zuo

Submitted to the Department of Mechanical Engineering

on May 6, 2006, in Partial Fulfillment of the

Requirements for the Degree of Master of Science in

Mechanical Engineering

ABSTRACT

Reported silica aerogels have a thermal conductivity as low as 15 mW/mK. The fragility of silica aerogels, however, makes them impractical for structural applications. The purpose of the study is to improve the ductility of aerogels while retain the low thermal conductivity of silica aerogels. We have established a new synthesis route, a 3-step sol-gel processing method. The method provides better control of the formation of aerogel structures. The produced silica aerogels show much improved ductility compared to conventional methods in literatures. Furthermore, the synthesized silica aerogels have thermal conductivities as low as about 9 mW/mK, which is the lowest in all reported solids. The ultra low thermal conductivity can be explained with nano-scale structures for the silica aerogels, which have been characterized using advanced techniques including BET and SEM.

We have further investigated and demonstrated the ability of enhancing mechanical properties of silica aerogels through structure modification using the proposed 3-step sol-gel processing method. The molecular-level synergism between silica particles/clusters and the doped functional materials inverts the relative host-guest roles in the produced aerogel composite, leading to new stronger and more robust low-density materials.

Thesis Supervisor: Taofang Zeng
Title: Principal Research Scientist of Mechanical Engineering
Thesis Co-Advisor: Gang Chen
Title: Carl Richard Soderberg Professor of Mechanical Engineering

Acknowledgements

First of all, I would like to express my gratitude to my thesis advisor, Dr. Taofang Zeng, for his supports and patience over the years. I deeply appreciate him for taking time out of his busy schedule to provide me his time and input. Secondly, I am grateful to my co-advisor, Professor Gang Chen, for his insightful guidance throughout the project. Without their encouragement, this thesis would never been accomplished.

I would also thank my labmates, including Yi He, Sheng Shen, Jinwei Gao, Shuo Chen, Qing Hao, for their research discussions and friendship, making my life enjoyable at MIT.

Also, I would like to thank Professor Lorna Gibson and Professor Leon Glicksman, for their collaboration and valuable advice. I would like to thank DuPont-MIT Alliance for their financial support.

Most importantly, I would like to thank my parents and my husband who have always been there for me along the way. I cannot thank them enough for their endless love and belief in me.

Dedicated to my beloved, Zhe!

Contents

List of Figures

List of Tables

1. Introduction

Silica aerogels, first produced by S.S. Kistler in 1931[1], have attracted more attention of researchers in various fields of science and technology. Silica aerogels have been referred as "frozen smoke" by their nebulous apprearance[2]. Silica aerogels will appear yellowish if a light source is viewed through them, and appear light blue under sunlight. Both phemonena are due to Rayleigh scattering, which results from micro porous structures. Typical silica aerogels consist of nano-sized open pores, with extremely low densities (0.003-0.35g/cm^3), large surface area(200-1600m^2/g)[3]. As a result of their unique microstructure, silica aerogels exhibit many fascinating physical properties, such as extremely low thermal conductivity, low acoustic velocity, low dielectric constant, tunable refractive index, etc.

Many fields of applications of silica aerogels have been reported based on the property of interest. The first application of silica aerogel was reported for the use in Cerenkov detectors based on the ability of tunable refractive index from 1.01 to 1.2 and this essentially helps to replace the use of compressed gas as the detection media [4]. Another interesting application of silica aerogels is for acoustic impedance matching devices due to their various and rather low acoustic impedance values from different combinations of sound propagation velocities and densities [5, 6]. Yet, the most promising application of silica aerogels is their use in thermal insulations. Transparent or translucent aerogels can be used as spacers in windows for day light applications and improve the use of solar energy, since the aerogels insulation is very effective [7]. The non-transparent aerogels have complementary applications where transparency is not required, such as refrigerators, heat storage devices and building insulations. Discussions for more versatile applications of aerogels can be found in many review papers [8-13].

The process to produce silica aerogels is called sol-gel process. In a sol-gel process,

a solution of silicate precursors undergoes changing from monomers to sol colloidal particles, which cross link into three-dimensional networks. The chemistry of sol-gel reactions, generation and aggregation of the particles or clusters have been well covered in books [14, 15] and several reviews [8-11, 13]. It has been known that the structure of gel network and the physical properties of silica aerogels strongly depend on the preparation of precursors' solutions and the chemical reaction conditions during sol-gel process. Currently, silica aerogels are produced from sol-gel process based on either 1-step acid or basic method, or 2-step acid-basic method. Because of the dependency of the hydrolysis and condensation reaction on the pH, sol particles will grow through derived models called reaction limited cluster aggregation (RLCA) under acid condition, or reaction limited monomer cluster growth (RLMC) under basic condition. Usually, polymeric-like network with small pores is formed under acid condition owing to the entanglement of less branched long chains, while, under basic condition, highly condensed structure with larger pores is formed from the aggregation of larger clusters. With the 2-step sol-gel method [16], a more deliberate control of the network structure has been realized, and production of silica aerogels with lower density and better transparency becomes possible.

Researchers have shown a lot interest on silica aerogels' physical propterties. An adverse characteristic property of silica aerogels is the brittleness, i.e., the compressive/tensile strength and elastic modulus of silica aerogels are very low. It is believed that the mechanical properties of silica aerogels are strongly dependent on the degree of network connectivity resulting from various sol-gel processing conditions. For example, it has been reported that silica aerogels prepared under acid or neutral catalytic conditions will appear twice stiffer than the aerogels prepared under base catalytic conditions [17]. Aging treatment after the gelation could change the gel network strength thus making gels more sustainable to the capillary stresses, and improving their mechanical properties.

Over the past decade, a number of researchers have tried to enhance the mechanical

properties of silica aerogels to make aerogels more ductile, and a couple of methods have been developed such as surface modification. More detail discussions on the topic can be found in Section 2.1.3. However, limited progress has been made, and it is desired to reinforce the mechanical properties of silica aerogels making them sufficiently strong for most applications.

On the other hand, the most attracting properties of silica aerogels are their extraordinarily low thermal conductivities. The total thermal conductivity of silica aerogels consists of three components: solid conduction, gas conduction and radiation [18]. Generally, solid conduction will increase as density increases, while, gas and radiation transports will decrease. In order to further lower the thermal conductivity of silica aerogels, evacuated silica aerogels have been investigated and a thermal conductivity of 0.010 W/m • K has been reported, comparing to 0.020 W/m • K with air[19]. Another approach is to reduce the radiation transport through addition of infrared opacifiers, such as carbon. For instance, carbon modified aerogels have been reported with a lower thermal conductivity of 0.0135 W/m • K and ~0.0042 W/m • K under vacuum condition [3].

To date, researchers only have some preliminary understandings of the chemistry-structure-properties relationships of silica aerogels, and most aerogels are still prepared empirically, and it is far away from chemically designed aerogel properties. Thus, the need for in depth understanding and better control of the chemical processes during gel network formation is expected. Furthermore, to promote and extend silica aerogels' applications, it is necessary to reinforce the mechanical properties of silica aerogels while retaining their fascinating properties, especially low thermal conductivities.

2. Background

2.1 The Fundamentals of Sol-Gel Silicates

2.1.1 Sol-Gel Processing

Sol-gel processing starts from the formation of sols. A sol is a colloidal suspension of solid particles in liquid phase, where the particles usually have sizes ranging from several nanometers to thousands of nanometers. A gel is a substance that contains continuous solid skeleton with enclosed continuous liquid phase [14]. Silicon alkoxides are the commonly used precursors with organic ligands attached to silica atom, such as tetramethyl orthosilicate(TMOS) and tetraethyl orthosilicate(TEOS). The first step to synthesize silica aerogels is to prepare sol particles' suspension, which is produced from chemical reactions of precursors. Then linkages among particles are formed leading to the formation of gel network that spans the entire liquid phase, so as to produce wet gels. The wet gels are then aged and dried, and finally silica aerogels are ready. Figure 2.1.1 is a schematic illustration of sol-gel process for silica aerogel synthesis.

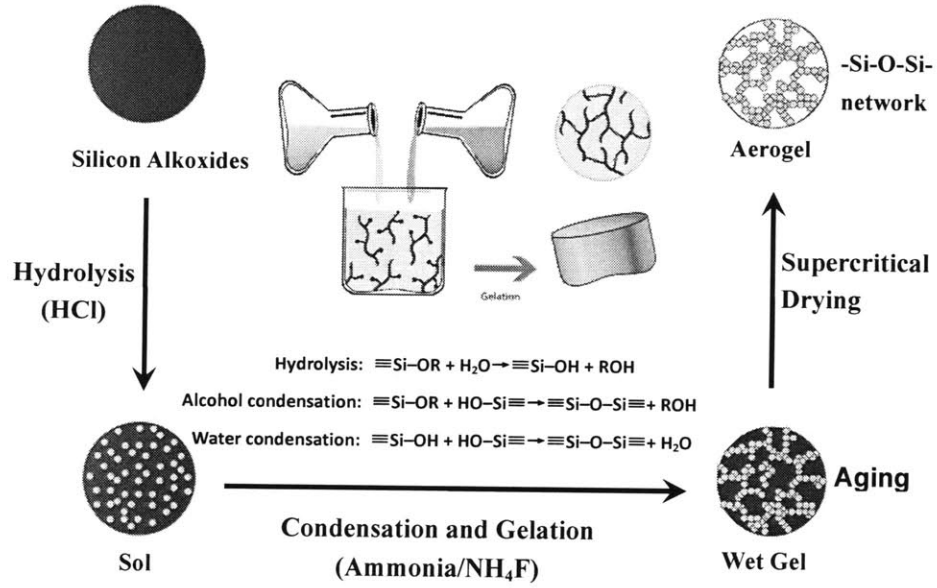

Figure 2.1.1 Schematic Illustration of Sol-Gel Process for Silica Aerogels

Fig.2.1.1 demonstrates the typical four steps for sol-gel processes: (1) hydrolysis of silica precursors, (2) condensation and gelation, (3) aging of the gel, and (4) drying of the gel.

2.1.1.1 Hydrolysis

During hydrolysis, precursors such as silicon alkoxides react with water to form silanols through the replacements of alkoxyl ligands(-OR) by hydroxyl groups(-OH). Depending on the type and the amount of catalysts being used, either complete hydrolysis or partial hydrolysis occurs. Complete hydrolysis means all –OR groups have been replaced by –OH, while partial hydrolysis produces molecules with composition of $Si(OH)_n$ $(OR)_{4-n}$. More detailed discussions on hydrolysis will be provided in Section 2.1.2.

2.1.1.2 Condensation and Gelation

Molecules from the hydrolysis step link together through condensation reactions, either by water condensation or alcohol condensation. These condensation reactions progress and lead to polymerization. Once the size of molecules reaches to the macroscopic level, gelation occurs. Gel point is the time when the last bond is formed that completes giant molecule[14]. For sol-gel process, different shapes of wet gels can be obtained by using various molds. Usually, monolithic aerogels have dimensions at least larger than millimeters. Factors that could affect sol-gel reactions and the resulting gel properties will be discussed in Section 2.1.2.

2.1.1.3 Aging of the Gel

It should be pointed out that chemical reactions do not stop at the gel point, and the wet gels need to be placed under aging for some period of time before being dried. For wet gels, the sol particles within the gel network are still reactive and could form further cross-links with the reactive sites in surroundings. The residue of the small sol particles either continues cross-linking among each other to form larger particles or reacts with the surface hydroxyl groups of gel networks. During aging, covalent

bonding replaces the non-covalent bonding which is resulted from weak forces such as Van der Waals forces, and wet gels shrink slightly.. The strength of the gel network is thus enhanced.

The wet gel networks have pore structures. During aging, some physical processes such as ripening or coarsening occur and favor pore structures with more rigidity [15]. Fig.2.1.2 is an example of the two connected particles within get network. For the individual particle, it has a positive surface curvature(r+), while the region around the narrow neck has a negative curvature(r-). A pressure gradient is generated across regions with different curvatures, resulting in different solubility of the material in those regions from the following equation:

$$S = S_0 \exp(\frac{2\gamma_{SL} V_m}{RTr}) \qquad (2.1.1)$$

Where, S is the curved surface solubility, S_0 is the flat surface solubility, γ_{SL} is the interfacial tension, V_m is the solid molar volume and T is the temperature, R is universal gas constant.

From Equation (2.1.1), it can be seen that the substance within particles has a higher solubility than the substance around narrow"neck" regions. Therefore, materials tend to accumulate toward to the narrow neck region, and the strength of pore walls is enhanced.

It should be noted that the aging step also provides the means to further modify the gel structures to tune the aerogels' functionalities. More discussions about structure modifications of silica aerogels can be found in Section 2.1.3.

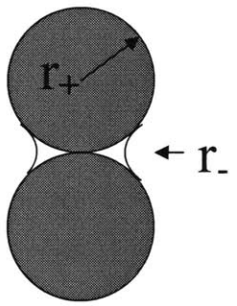

Figure.2.1.2 Curvature of particles and narrow "neck"

2.1.1.4 Drying of the Gel

Wet silica gels are porous materials with liquid inside the pores. When liquid is removed by evaporation or boiling, the capillary stresses are so strong that the gel networks shrink significantly and the pore structures collapse. Several methods have been developed to overcome the structure changes during drying. One is to add surfactants into the liquid to reduce the interfacial energy and to decrease the capillary stress. Zarzycki[20] has demonstrated that both cracking and shrinkage could be reduced by addition of surfactants. Another method is the use of drying control chemical additives (DCCA), such as formamide (NH_2CHO), oxalicacid (HOOCCOOH), dimethyformide (DMA) and acetonitrile. Formamide enables the gels to be harder,, and allows the pores to be larger and more uniform pore distributed [21]. Additionally, coarsening during aging step could also be promoted by hydrolysis of formamide[22]. The two methods help the reduction of gel shrinkage and cracking. However, the additives involved by these two methods are very difficult to remove and make the aerogel unhygienic..

Kistler[1] invented a drying method, supercritical drying, a widely used method in current sol-gel process. The fundamental mechanism for the method is that the capillary stresses could be avoided by removing the liquid from the pores under the condition above the liquid critical point (Tc, Pc), where there is no distinction between liquid phase and vapor phase and thus no capillary stresses in the pores. Table 2.1.1 lists the critical points for several solvents [14]. Nowadays, supercritical carbon dioxide with much milder required drying conditions (critical point of CO_2 is 31.1 ^{0}C at 1070 psi.) is the most commonly used drying liquid. Figure 2.1.3 is the carbon dioxide pressure-temperature phase diagram[23]. In our study, a homebuilt supercritical CO_2 drying system has been employed to dry all the wet gels.

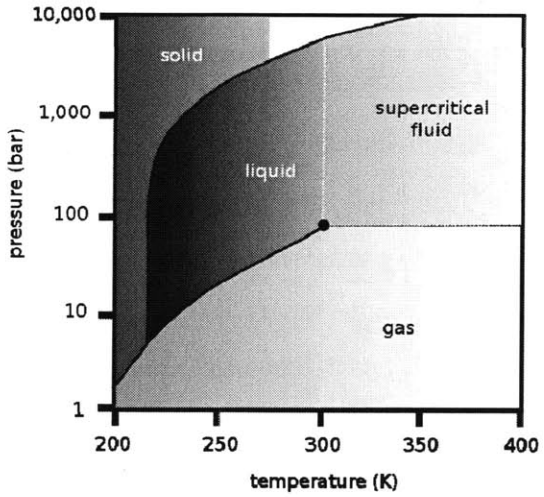

Figure 2.1.3 Carbon Dioxide Pressure-Temperature Phase Diagram

Table 2.1 Critical Points of Selected Solvents.

Substance	**Formula**	***T c* (^{0}C)**	***P c* (MPa)**
Carbon Dioxide	CO_2	31.1	7.36
Freon 116	CF_3CF_3	19.7	2.97
Methanol	CH_3OH	240	7.93
Ethanol	C_2H_5OH	243	6.36
Water	H_2O	374	22.0

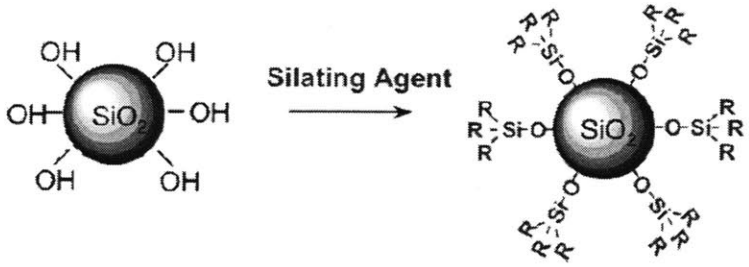

Figure 2.1.4 Silylation of Silica Aerogels

The high operating pressure during supercritical drying requires the drying system with specific design so as to avoid any leak, which is costly. Recently, ambient pressure drying has been investigated. In order to realize ambient pressure drying, pore surface modification and gel network strengthening have to be performed in advance to minimize the effects of capillary stresses. It should be emphasized that ambient pressure drying can only be performed for hydrophobic aerogels. In this case, surface modification should be conducted. Silylation is such a typical process.

In the process, the hydroxyl groups(-OH) located on the surface of aerogel are replaced by-OR (R= alkyl group) functional groups, yielding aerogels hydrophobic (Figure2.1.4). Some typical silylating agents are: methyltrimethoxysilane(MTMS), methyltriethoxysilane (MTES), dimethylchlorosilane (DMCS), trimethylethoxysilane (TMES), ethyltriethoxysilane (ETES), phenyltriethoxysilane (PTES), trimethylchlorosilane (TMCS), and hexamethyldisilazane (HMDZ). Kang and Choi[24] successfully synthesized silica aerogel monoliths under ambient pressure drying using TMCS as the silylating agent. Rao[25] prepared silica aerogels by using hexamethyldisilazane(HMDZ) as silylating agent with improved properties, such as lower density, higher hydrophobicity, lower thermal conductivity, higher porosity and higher transparency. Wei[26] synthesized ambient pressure dried silica aerogels with TMCS as silylating agent and hexane as solvent from multi-step surface modification to reduce the volume shrinkage, increase the monolithicity and porosity, and lower thermal conductivity. Since silylation is usually conducted in organic solvent environment, solvent exchange is necessary. The usage of large amount of organic solvent, and much longer preparation time for solvent exchange and surface modification together significantly increase the cost of ambient pressure drying process. Freeze drying is another way to avoid the capillary stress during the removal of solvent from wet gel structures. In this case, solvents with low expansion coefficient and high sublimation pressure are needed. During freeze drying, solvent in the pores is frozen becomes solid, which is then removed under vacuum sublimation. However, it is very

difficult to obtain monolithic silica aerogels under freeze drying, as the solvent recrystallizes inside the gel networks in freezing drying. These crystals expand and stretch, which cause the surrounding gel network, to break. Thus, flakes or fibers of silica aerogels are produced from freeze drying [27-29] Nonetheless, if the mechanical properties of silica aerogels can be improved favorably, freeze drying could become applicable for preparing monolithic silica aerogels.

2.1.2 Chemical Reactions of Sol-Gel Silicates

As discussed in preceding section, the two main chemical reactions for sol-gel process are hydrolysis and condensation, which are usually performed with catalysts under acidic or basic conditions(see Figure 2.1.1). Tetra functional alkoxides such as tetramethoxysilane (TMOS) and tetraethoxysilane (TEOS) are commonly used precursors for synthesizing silica aerogel,. During the hydrolysis reaction, alkoxide groups (-OR) are replaced by hydroxyl groups (-OH). Then, silanol groups link with each other to form siloxane bonds (Si-O-Si) while releasing water or alcohol during condensation. Since alkoxysilanes are not miscible with water, co-solvent (such as alcohol) is added to prevent phase separation. But, it should be noticed that, since alcohol are by-products of hydrolysis step, once hydrolysis has proceeded, the initial phase separated system could also be homogenized even without addition of extra alcohol.

A lot of investigations have been performed to study how reaction conditions (H_2O:Si ratio R, catalyst type and concentration, solvents, aging time and temperature, drying conditions, etc.) affect the characteristics and properties of the synthesized sol-gel products. In this section we focus on discussions of the effects of H_2O: Si ratio R, catalysts and solvents. Table 2.2 summarizes some typical sol-gel syntheses for silica aerogels [14].

From Table 2.2, it can be seen that there are generally two types of methods for a sol-gel process: the 1-step acid or base method, and the 2-step acid-base method. The

1-step acid method for sol-gel process with R=1 can be used to produce primarily linear or weakly branched structures, while the 1-step base method produces particles with highly branched structures [30](also see Figure 2.1.5).

Table 2.2 Sol-Gel Compositions for Bulk Gels, Fibers, Films, and powders.

	mole %					
SiO_2 Gel Types	**TEOS**	**EtOH**	**H_2O**	**HCl**	**NH_3**	**H_2O:Si ratio R**
Bulk						
1-step acid	6.7	25.8	67.3	0.2	-	10
1-step base	6.7	25.8	67.3	-	0.2	10
2-step acid-base						
1st step-acid	19.6	59.4	21.0	0.01	-	1.1
2nd step-acid	10.9	32.8	55.7	0.6	-	5.1
2nd step-base	12.9	39.2	47.9	0.01	0.016	3.7
fibers	11.31	77.26	11.31	0.11	-	1.0
films	5.35	36.23	58.09	0.35	-	10.9
Monodisperse, Spheres	0.83	33.9	44.5	-	20.75	53.61

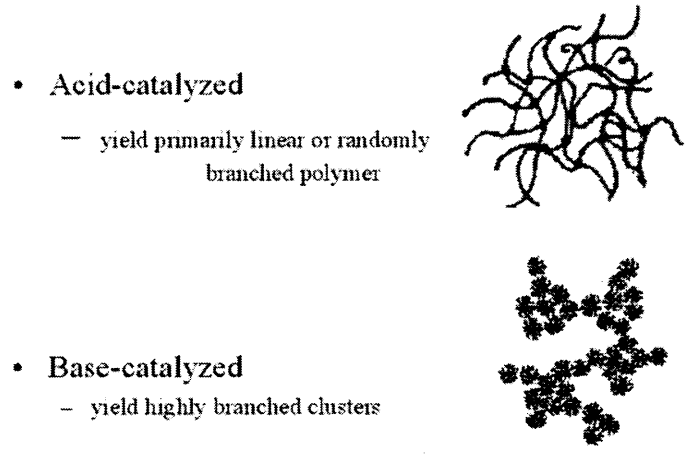

Figure 2.1.5 Inorganic network structures from sol-gel reactions under acidic or basic conditions [36]

2.1.2.1 Effects of H_2O: Si ratio (R)

Since water is a by-product from the condensation step, theoretically, R=2 in the initial condition is sufficient for hydrolysis. Previous studies have shown that the R value ranging from 1 to 50 produces various gel structures. Sakka [31-33] found that hydrolysis of TEOS with R value of 1~2 and with catalyst under acidic condition (0.01M HCl) yields viscous and spinnable sol solutions. Spinnable solutions exhibit a power law dependence of the intrinsic viscosity as a function of the number average molecular weight, as demonstrated by Eq. (2.1.2.):

$$[\eta] = kM_n^{\alpha} \tag{2.1.2}$$

where, $[\eta]$ is the intrinsic viscosity, M_n is the molecular weight, and , k and α are constants for a given polymer-solvent system.

In the above equation, when α ranges from 0.5 to 1.0, it indicates linear or chain molecules [34]. While, the reaction solution with R values larger than 2 produce unspinnable solution, and values of α ranging from 0.1~0.5 indicate spherical or disk shaped particles [31,33]. SiO_2 powders were prepared from hydrolysis of TEOS with R values varying from 20~50 under basic condition [35].

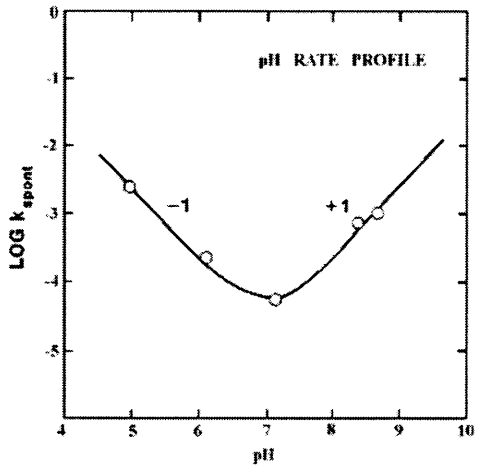

Figure 2.1.6 pH rate profile for the hydrolysis in aqueous solution [38]

2.1.2.2 Effects of Catalyst

pH

Even though sol-gel reactions can occur without catalysts, they can be faster and more complete when catalysts are employed. Mineral acids(HCl) and ammonia are commonly used catalysts. Other reported catalysts are acetic acid, KOH, KF, NH_4F and HF[37].

For hydrolysis reactions, Pohl and Osterholtz[38] studied how the hydrolysis rate of γ -glycidoxypropyltrialkoxysilane related to pH in aqueous solution(see Figure 2.1.6).It shows that the hydrolysis can be catalyzed by either hydronium ion when pH<7 or hydroxyl ion when pH>7. McNeil[39] also observed the same relation for the hydrolysis of tris(2-methoxyethoxy)phenylsilane. Aelion[40, 41] found that the rate and the extent of hydrolysis primarily depended on the strength and concentration of the acid or base, and the temperature or solvent was only secondarily important. By plotting the hydrolysis rate constant versus acid concentrations, only a slope was observed with either pH<7 or pH>7, indicating that the hydrolysis reaction was first-order under both acid and basic conditions.

Aelion[40] investigated the hydrolysis of TEOS under both acid and basic conditions using different solvents including ethanol, methanol, and dioxane. It was found that under basic condition, when the concentration of TEOS, increase, the hydrolysis reaction is changed from a simple first-order to a more complicated second-order reaction, especially with weaker bases, such as, ammonium hydroxide and pyridine. Thus, compared to acidic conditions, the hydrolysis kinetics under basic condition is more solvent dependent.

For condensation reactions, Engelhardt [42] proposed that typical condensation products consequently consist of monomer, dimer, linear trimer, cyclic trimer, cyclic tetramer, and higher order rings. Thus, during the condensation, there exists equilibrium between depolymerization (ring opening) and polymerization of monomers with the

oligomeric species, and the equilibrium is dependent on the environmental pH. With pH<2, the condensation rates are proportional to the [H^+] concentration. Since the solubility (see Figure 2.1.7) of silica is extremely low, the obtained gel networks are composed of extremely small silica particles (usually less than 2nm)[14]. When pH is 2~6, condensation preferentially occurs between higher molecular weight particles and monomers or the less condensed particles. Thus, dimerization is less likely to occur. However, once dimers are formed, they quickly react with monomers to form trimers, which in turn react with monomers to form tetrameters. Then chains formation and gel networking occur by the addition of lower molecular weight particles to highly polymerized particles and aggregation of high molecular weight particles/clusters. The solubility of silica in this pH range is still relatively low and the formed gel networks are mostly composed of particles with 2-4 nm in diameter [43]. When pH >7, the sequence of polymerizations is the same as pH 2~6. Howevre, in this pH range, particles are ionized and mutually repulsive, thus, particles are preferentially growing through the addition of monomer to highly polymerized particles rather than aggregation among larger particles/clusters. In addition, the solubility of silica is much greater, and smaller particles are even more soluble than larger particles, thus the gel networks are primarily composed of larger size particles, which eventually lead to the formation of gels with large pores [14].

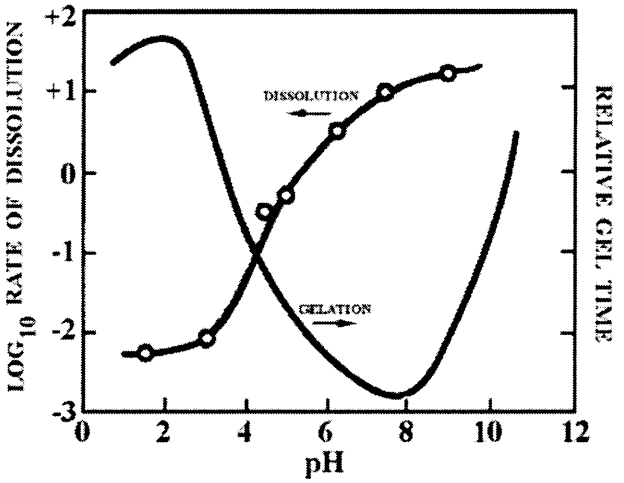

Figure 2.1.7 Dissolution rate and relative gel time as a function of pH.

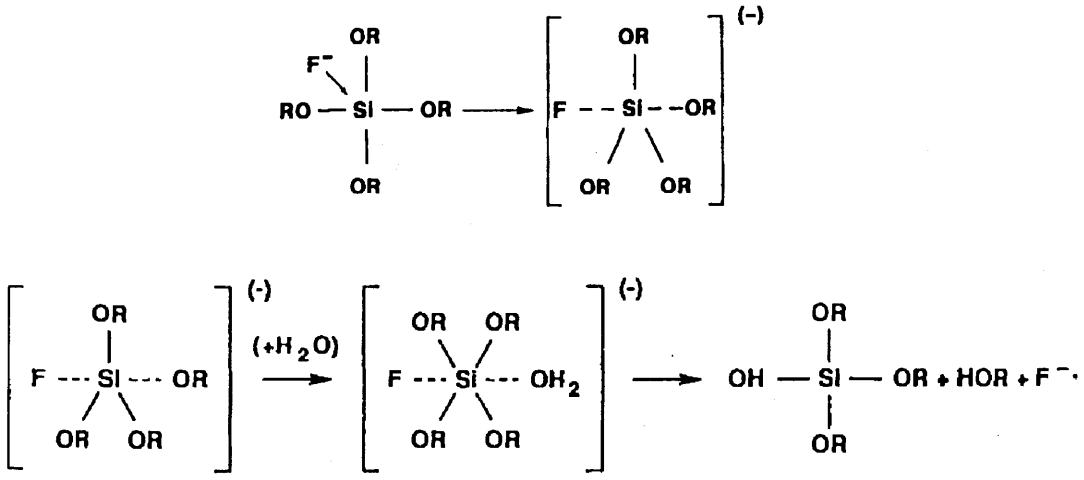

Figure 2.1.8 F^- catalyzed sol-gel reactions

F^-

The F^- has a similar size as OH^-. However, with F^-, the silicon coordination number is increased up to five or six. Hydrolysis using HF produces gels whose properties are similar to those of base catalyzed gels. Corriu[44] demonstrated that for F^- involved hydrolysis, the first step is the formation of a pentavalent intermediate that repulses and

weakens the adjacent Si-OR bonding. Then the next step of nucleophilic attack of water leads to the substitution of –OR with –OH (see Figure 2.1.8).

Previous researches have also shown that F^- has remarkable catalytic effects on the rate of condensation reactions. Rabinnovich and Wood[45] proposed that the mechanism for F^- catalyzed condensations involves the displacement of OH^- with F^-, causing localized attractions to surrounding silanol groups, thus promoting the condensations. Also, since F^- is more electron-withdrawing than OH^-, so the replacement of F^- with OH^- will cause reduction in the electron density of Si, thereby making nucleophilic attack from the other OH^- groups much easier to happen.

2.1.2.3 Effects of Solvent

The alkyl groups in silicon alkoxides are hydrophobic, causing phase separation during the initial mixing stage of precursors. Thus, solvents are added to prevent the happening of phase separation. It has shown that the addition of solvent will also influence the reactions kinetics. Solvents are classified as polar or non polar and as protic(containing labile proton) or aprotic. Polarity, dipole moment and availability of labile protons are most important characteristics of solvents. Polar solvents, such as water, alcohol or formamide, are normally used to solvate tetra functional silicon alkoxides in sol-gel processing. Ether alcohols, such as methyl alcohol and ethyl alcohol, exhibit both polar and nonpolar characters and are often used in solutions containing both polar and nonpolar substances.

From the discussions in Section 2.1.2.2, hydrolysis can be catalyzed by both hydronium ion when pH<7and hydroxyl ion when pH>7. It is also known that, hydrogen bonding can occur between solvent molecules and hydromium ions under acid catalytic condition, or between solvent molecules and hydroxyl ions under base catalytic condition. The hydrogen bonding thus adversely affects the hydrolysis. Hence, aprotic solvents that barely form hydrogen bond with hydroxyl ions under base condition enable the hydroxyl ions more nuclephilic, whereas, protic solvents under

acid condition make hydronium ions more electrophilic[46]. Therefore, hydrolysis can be accelerated with increasing concentration of aprotic solvent under base-catalyzed condition, but decelerated with protic solvent under acid-catalyzed conditions.

After hydrolysis, the silanols are either deprotonated or protonated for condensation. The deprotonated silanols are facilitated to form hydrogen bonding with solvent molecules in protic solvents, so are the protonated silanols with solvent molecules in aprotic solvent. Therefore, increasing protic solvent concentration can decrease the condensation rate under base-catalyzed condensations, and increase the reaction rate of acid-catalyzed condensations. Whereas, increasing aprotic solvent concentration can increase the base-catalyzed condensation rate and decrease the acid-catalyzed condensation rate [14].

Another important effect of solvent is the ability to promote depolymerization during condensations. Iler[47] reported that, when depolymerizations are suppressed during condensations, crosslinked gel networks consisting of branched polymeric particles/clusters are formed. Whereas, with depolymerizations, highly condensed particles/clusters are produced, in which yields relatively higher dense and rigid gel structures. This can be further explained as follows. Under base-catalyzed condensations, the aprotic solvent molecules are unable to form hydrogen bonding to OH^-, enable OH^- to be even stronger nucleophile, which promotes restructuring and produces more highly condensed particles.

2.1.3 Structure Modifications of Silica Aerogels

Silica aerogels have a extremely high surface area(~1000m^2/g) and high porosity (>90%). Modification to aerogel structure is equivalent to surface modification. Generally, there are two different kinds of methods for surface modifications of silica aerogels: (1) Surface derivatization method and (2) Co-precursor method [48]. For surface derivatization method, wet silica gels are formed first, and then put into aging solutions containing a mixture of solvent and the surface-modifying agent. Then mass

transfer takes place through infiltration process, which leads to cross-linkings between silica skeleton and surface-modifying agent. Usually, a huge amount of solvent and a long process time are needed to achieve complete solvent exchange and subsequent surface modifications, which is very costly. For co-precursor method, the surface modifying agent is added into the sol as co-precursor before gelation. Compared to the surface derivatization method, the co-precursors method produces gels with more uniformly modified surface and higher integrity in bulk properties, and takes a shorter time [49,50].

2.1.3.1 Surface Derivatization Method

Surface derivatization through liquid-phase crosslinking between silica gel skeleton and polymer cross-linkers has dramatically improved the strength of silica aerogels. Leventis and co-workers have proposed a method to do so[51-53]: the wet silica gels are soaked into solutions containing diisocyanates-crosslinking agents, and diisocyanates react with hydroxyl groups located on surface of silica particles with the formation of carbamate bonds, which commonly exist in the polyurethane skeletons(see Figure2.1.9). After supercritical drying, the obtained polymer cross-linked aerogels are much stronger than typical silica aerogels. They can be bended without breaking. Other reported polymer cross-linkers are epoxides [55, 56] and polystyrene[57-59]. Gupta and Ricci[55], encapsulated the silica particles in epoxy resin by immersing wet silica gels into a resin-solvent mixture. The obtained aerogel/epoxy composites are reported to have compressive failure strain of over 25%. Nguyen [57] examined styrene cross-linked silica aerogels with much improved elastic behaviors. It has been demonstrated that the styrene-modified silica aerogels can recover nearly 100% of their length after compression to 25% strain twice. Although silica aerogels with improved mechanical strength and flexibility have been produced through incorporating organic cross-linkers, several disadvantages have also been noticed, such as, increased density, decreased surface area, and reduced thermal insulation ability.

In addition to liquid phase cross-linking, structure modifications of silica aerogels can also be conducted after they have been already dried. Chemical Vapor Deposition (CVD) or Atomic Layer Deposition (ALD) can be employed to deposit a conformal polymer coating throughout the pore surface of silica aerogels. Boday [60] demonstrated the principle by depositing ambient-temperature CVD of methyl cyanoacrylate onto silica aerogels and observed that 32 times increase in compressive strength was obtained with only 3 times increase in density.

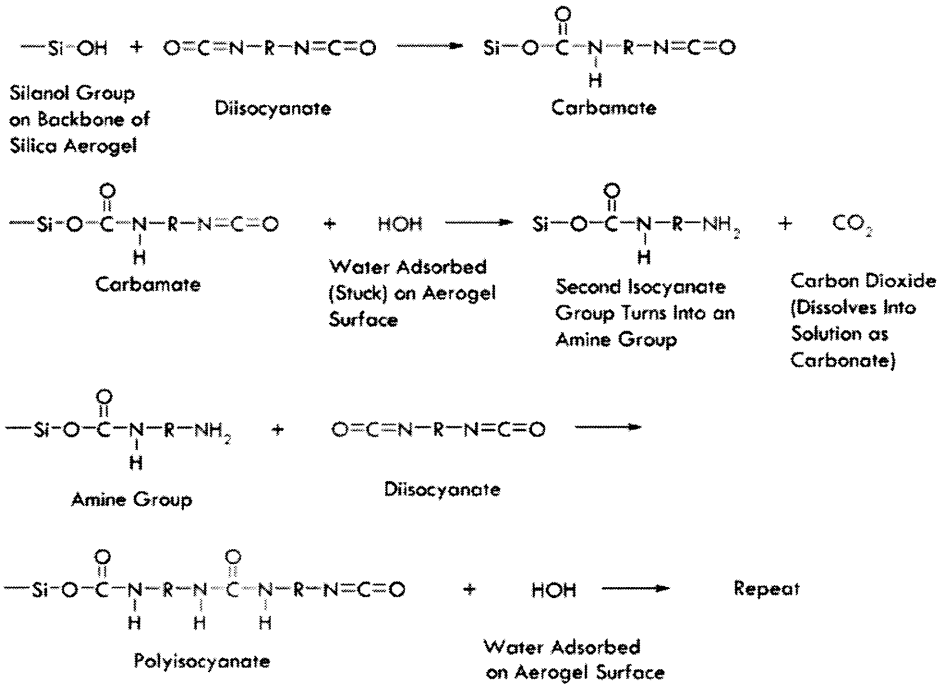

Figure 2.1.9 Chemical reactions that underly crosslinking of silica aerogels with a conformal polyisocyante coating[54]

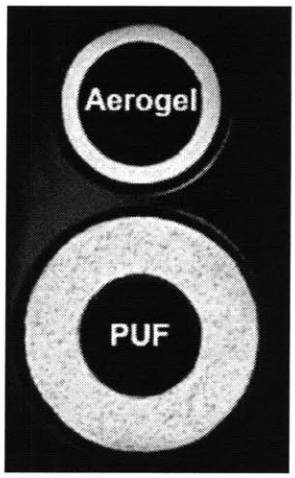

Figure 2.1.10 Cross-sections of pipeline insulations using fiber-reinforced aerogel blankets and polyurethane foam (PUF)[54]

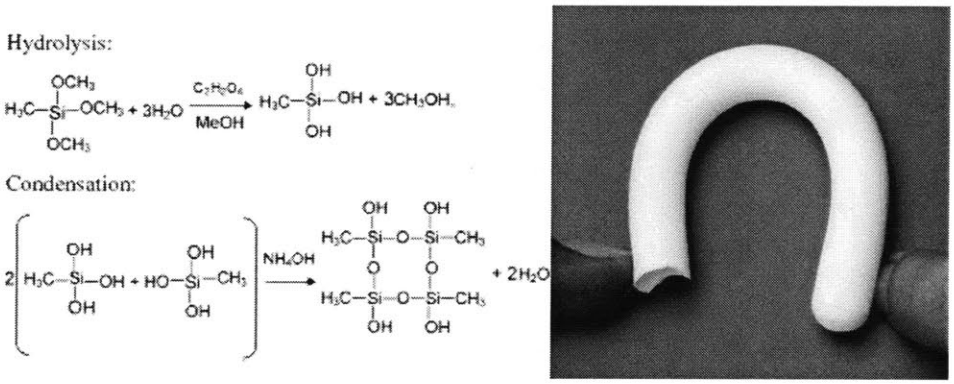

Figure 2.1.11 Sol-gel reactions and silica aerogels with high flexibility prepared using MTMS

2.1.3.2 Co-Precursor Method

Incorporating microfibers into the precursor sols before gelation is another method to increase both of compressive strength and modulus of silica aerogels. Finlay [61] found that the incorporation of short-cut natural fibers (~2mm in length) with aerogels dramatically increased the mechanical properties of aerogels. It is reported that with 5 wt % fiber loadings, the compressive strength and modulus could be both increased by

as much as 5 times, while the bulk densities were increased by less than 2 times. They claimed that the woven-like structure composed of clay aerogel "warp" and fiber "weft" materials seemed to be responsible for the enhancements of the mechanical properties.

Aspen Aerogels has also fabricated fiber reinforced silica aerogels [62-64]. Their production of mechanically robust, flexible aerogel blankets with lower thermal conductivity(~0.014W/mK) are made of both inorganic and organic aerogels supported by meshes of polyimides (i.e., Nylon®), glass fibers, and many other materials. One of their products has been used in sub-sea oil pipelines insulation, and can significantly reduce the size of outer pipes and costs for shipping comparing to polyurethane foams (see Figure2.1.10). However, unlike monolithic aerogels, the aerogels' blankets consist of silica granules and the continuously releasing aerogels dust in processing is hazardous.

Cellulose is a biodegradable, renewable resource, and is taken as "green". Cellulose modified silica aerogels produced by addition of cellulosic materials into precursors' sol, have been attracting increasingly attention,. Sequeira [65,66] worked on the preparation of cellulose/silica hydrid composites by incorporating silica into cellulosic materials, such as bleached kraft pulp. They found that using heteropoly acid as catalyst yields a higher efficiency for the addition of silica precursors (TMOS or TEOS) to cellulosic structure. However, their reported thermal conductivity of the final hybrid composite with roughly 40wt%~60wt% of silica incorporated is extremely high, ~0.15W/mK, which is attributed to the poor thermal insulation ability of the cellulosic contents.

Compared with tetrafunctional silicon alkoxides, trifunctional silicon compounds, such as MTMS (methyltrimethoxysilane) and MTES (methyltriethoxysilane), has a bond terminated by a methyl or ethyl group to the silicon atom. Therefore, during sol-gel reactions, each silica precursor molecule only has three possible oxygen bridges

connected to other silicon atoms. Rao[67-72] prepared silica aerogels using trifunctional alkoxides as precursors or co-precursors through a two-step acid–base method for sol–gel process, and obtained highly flexible silica aerogels (see Figure 2.1.11). The presence of non-polar alkyl groups (i.e. methyl) attached to the silica polymer chains minimize the inter-chain cohesion and make the gel particles with reduced overall bonding, leading to the formation of elastic and flexible three-dimensional gel network. Moreover, the methyl or ethyl groups attached to each silicon atom contribute to the superhydrophobicity. Kanamori and co-workers [73, 74] have syntheized silica aerogels with high transparency from MTMS, where they used surfactant to prevent macroscopic phase separation. However, the thermal conductivity of these aerogels were again found to be around 0.095W/mK, much higher than regular silica aerogel(0.015W/mK) [67].

2.2 Physical Properties of Silica Aerogels

2.2.1 Elastic Property

The elastic modulus of silica aerogels has been studied and measured using conventional three-point flexural techniques. It has been found that the elastic modulus has a strong relationship with pore volume, pore shape, skeleton density and bulk density. Woignier [75, 76] investigated the elastic properties of silica aerogel prepared from TMOS catalyzed under various conditions, namely, acidic, basic, or neutral. The data measured by three-point flexural method have been fitted and plotted (see Figure 2.2.1). The figure shows a power law relationship between aerogel's bulk density and Young's modulus:

$$E \propto \rho^{3.7\pm0.3} \qquad (2.2.1)$$

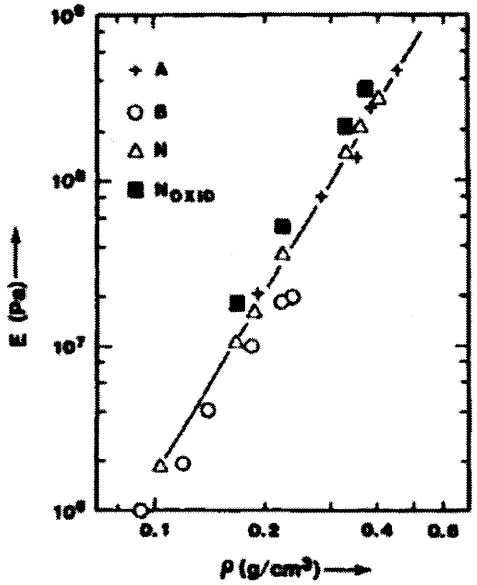

Figure 2.2.1 Log-log plot of Young's modulus vs. bulk density for aerogels prepared from TMOS hydrolyzed under neutral(N), acid(A) or base(B) conditions. Oxidation treatment (N_{OXID}) was at 500 ^{0}C[75]

This scaling behavior is similar to that expected by percolation theory:

$$E \propto \rho^{T/\beta} \tag{2.2.2}$$

where ρ is the density of the infinite cluster, T and β are percolation exponents related to the elasticity and gel fraction, respectively. However, percolation theory doesn't account into the shrinkage occurred from syneresis during aging and supercritical drying, so it may only qualitatively describe the elasticity by the gel point [76].

In most mechanical property models of porous materials, Young's modulus is only dependent on the bulk density (and pore shape for some cases)[77]. For open-cell foam, the Young's modulus has the following relationship with bulk densities:

$$E / E_S \approx (\rho / \rho_S)^2 \tag{2.2.3}$$

where, E and E_S are the modulus for foam and cell-wall, ρ and ρ_S are foam density and cell-wall density respectively. However, for silica aerogels, the Young's modulus also depends on the sol-gel synthesis conditions. From Figure 2.2.1, it is

apparent that for the same bulk density values, base-catalyzed conditions lead to relatively lower E than acid or neutral catalyzed conditions. Woignier [76] attributed the lower E of the base-catalyzed silica aerogels to larger primary particles with lower particle-particle connectivity, whereas, acid and neutral-catalyzed conditions resulted in the aerogels primarily composed of smaller particles leading to higher particle-particle connectivity, and increased aerogel's stiffness.

2.2.2 Thermal Conductivity

With a high porosity (>90%), large surface area (~1000m^2/g) and a nanoporous structure, silica aerogels are excellent insulating materials having a thermal conductivity much lower than the still air (0.025W/mK). Thermal conductivity of aerogels arises from three sources: conduction in solids, conduction in gases in the pores, and radiation through the entire structure. The solid thermal conduction is limited by the extremely low connectivity between particles. Similarly, the gas conduction is suppressed as the mean free path (average distance traveled between collisions) of gas molecules inside aerogels is significantly limited by the nanosized pores, and the interstitial gas molecules collide with the pore walls more frequently than they collide with each other. The radiative conductivity is also lower because of its smaller solid content and higher surface area. Yet at higher temperature, radiative conductivity increases dramatically and becomes the dominant thermal transport mode of silica aerogels.

Hrubesh and Pekala[78] examined the three major thermal transport modes of aerogels and proposed that a thermal resistance value of R=20 per inch could beome possible by optimizing the synthetic and engineering approaches of making aerogels. Here, the thermal resistance R -factor is the inverse of the thermal conductivity in English units (i.e., BTU • in/h • ft^2 • °F), and it is numerically equal to 0.1443 divided by the thermal conductivity in MKS units (i.e., W/m • K).

Solid conductivity $\lambda_s^{'}$ in aerogels is empirically expressed by [79]:

$$\lambda_s' = \frac{\rho' v'}{\rho_s v_s} \lambda_s \tag{2.2.4}$$

where ρ' and ρ_s are the densities of the aerogel and the full solid respectively. v' and v_s are their respective longitudinal sound velocities, and λ_s is the thermal conductivity of the solid. The most important terms for solid conductivity is the ratio $\lambda_s / \rho_s v_s$ in Equation (2.2.4), which can be minimized by proper selection of the solid used to make the aerogel. That implies that, one should use a high density material that has a low intrinsic thermal conductivity and a high sound velocity to achieve low thermal conductivity.

Gas conductivity λ_g' in aerogels can be approximated by [80]:

$$\lambda_g' = \frac{\lambda_{g0} \bullet (1 - \rho'/\rho_s)}{1 + \alpha \bullet Kn} \tag{2.2.5}$$

where λ_{g0} is the thermal conductivity of the gas in the pores, α is a constant depending on the gas (~2 for air), and K_n is the Knudsen number, given by the ratio of the mean-free path for gas molecules, l, and the average pore size, Φ, of the aerogel[81]. Equation (2.2.5) shows that the pore size, which affects the Knudsen number, is an important factor in reducing the gaseous contribution to the conductivity. Smaller average pore size increases the Knudsen number and thus decreases the gaseous thermal conductivity.

Radiative conductivity λ_r' in aerogels is approximated by[82]:

$$\lambda_r' = \frac{16 \bullet n^2 \bullet \sigma \bullet T_r^3}{3 \bullet \rho' \bullet K_s / \rho_s} \tag{2.2.6}$$

where σ is the Stephan-Boltzmann constant (σ = 5.67 X 10^{-8} W/m^2 K^4), n is the refractive index (~1 for aerogels), T_r is the mean temperature within the aerogels, and

K_S is the extinction coefficient for the solid. The extinction coefficient is the inverse of the mean free path for photons, l', in the material. Most of the solid materials are optically thick, in which l' is much smaller than the geometrical thickness. However, many porous materials are not optically thick, especially at infrared (IR) wavelengths, such as aerogels. Thus, the radiative conductivity becomes even more significant at very low densities and at high temperatures. Clearly, to reduce the radiative conduction, adding materials that has strong infrared radiation absorption into silica aerogels can significantly increase the extinction coefficient for silica and thus also reduce the λ_r'.

Based on the above analysis, all contributions to the total thermal conductivity of silica aerogels are dependent on the density. Figure 2.2.2 schematically shows the contribution of these thermal transport modes depending on the bulk density. Clearly, the solid conductivity increases with increasing density, while, gas and radiative transports decrease with increasing density. The minimum total thermal conductivity occurs at a density of about 0.15g/cm^3 for the specified aerogels [18].

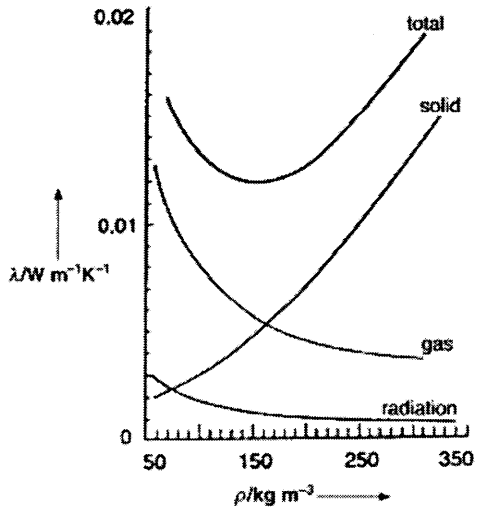

Figure 2.2.2 Thermal conductivity of silica aerogels with contributions from gas, solid and radiation transport depending on the bulk density [18]

Other factors including temperature, aerogel structure, interstitial gas types, pore structure could also affect the contributions. This creates a rather complicated set of circumstances, and makes it difficult to broadly generalize aerogels' thermal properties. Yet researchers in this field have developed some strategies to lower the thermal conductivity of aerogels such as (1) employing organic or inorganic materials with low intrinsic solid conductivity, (2) reducing the average pore size within aerogels, (3) increasing the infrared extinction in aerogels through good IR absorbers and (4) conducting partial evacuation and sealing of aerogel monoliths.

2.3 Applications

2.3.1 Thermal Insulation

Silica aerogels hold the lowest thermal conductivity record in solid materials. The most attracting and promising application for silica aerogels is thermal insulation. Aspen Aerogels produces a family of products based on fiber reinforced silica aerogels, such as Spaceloft™, Pyrogel®, and Cryogel™, for fire protections, pipeline insulations, et al. Figure 2.3.1 and Figure 2.3.2 show the thermal conductivity and the corresponding thermal resistance comparisons between those silica aerogels' products and other conventional insulation materials at ambient temperature and pressure[62]. However, since their products are produced from aerogel granules, two problems including significant volume shrinkage and consistently rerelease of silica dust during applications are still bothering Aspen Aerogels' scientists. Thus, monolithic silica aerogels with lower thermal conductivities (<0.01W/mK) and higher R-value, and with a mechanical robust and high environmental stability are desired to enhance energy efficiency of thermal insulation.

2.3.2 Energy Absorbing Materials

Silica aerogels are low-density materials and brittle. During the collapse of the solid

network, the impact force spreads gradually over the bulk for a longer time. Additionally, silica aerogels are an open-cell porous material. During impact, gases rapidly pass through the pore network composed of narrow pores (20~50nm) and absorb a considerable amount of energy by frictions. Therefore, the energy of impact is damped by the aerogels through the collapse of their solid structure and the release of gas from within the pores.

In comparison, many organic foams generate a significant amount of rebound during impact, which can do further damage to the object being protected. Figure 2.3.3 shows a plot of deflection vs. time for silica aerogel and polystyrene upon impact which clearly demonstrates the differences in rebound [83]. Silica aerogels with almost no bouncing effect are considered as an ideal candidate when developing materials for safety and protective devices.

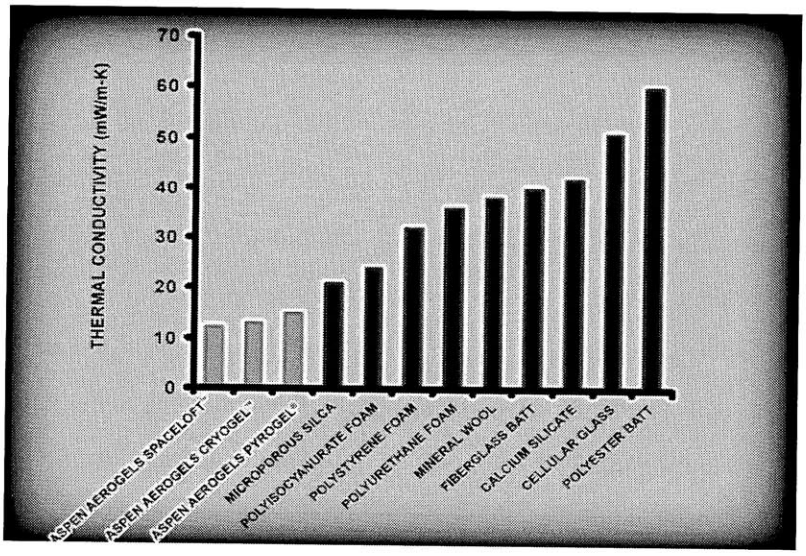

Figure 2.3.1 Thermal conductivity comparison between Aspen Aerogels' products and other conventional insulation materials at ambient temperature and pressure

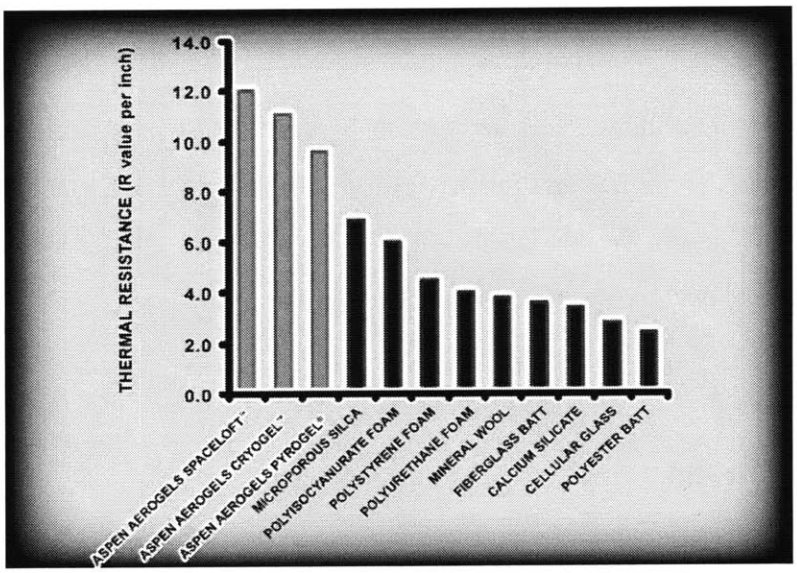

Figure 2.3.2 Thermal resistance comparison between Aspen Aerogels' products and other conventional insulation materials at ambient temperature and pressure

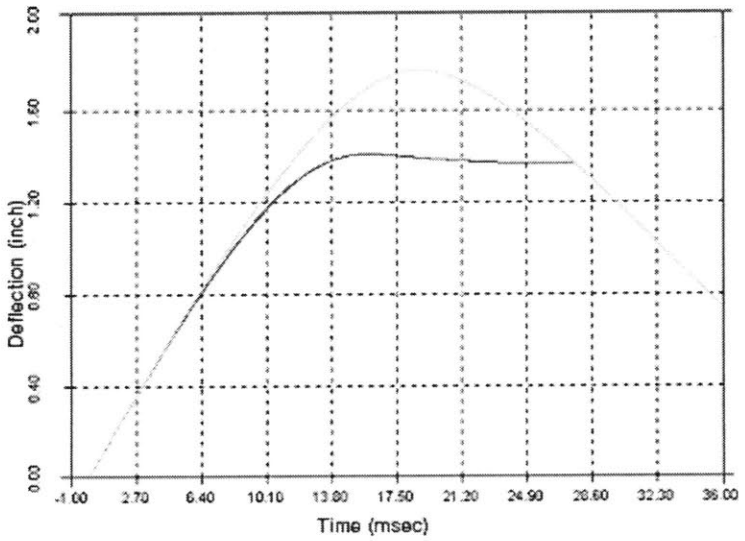

Figure 2.3.3 Deflection vs. time for silica and polystyrene during an impact.

2.3.3 Others

Other applications of silica aerogels have been reported based on specific property of interest. Monolithic silica aerogels have been used in high energy physics in

Cherenkov radiation detectors on the basis of their tunable refractive indices[4]. Low acoustic impedance, resulting from silica aerogels' low densities as well as low velocity of sound (100 m/s), allow silica aerogels to be very useful in acoustic impedance matching devices [6]. Silica aerogels have found applications as inertial confinement fusion (ICF) targets in thermonuclear fusion reactions [84], high efficient radioluminescent devices in place of fragile vacuum systems [67, 85].

2.4 Motivations

In summary, silica aerogels are open-cell porous materials with extraordinary low thermal conductivity [3],. Thus, silica aerogels are desired for structural thermal insulations. However, the fragility of silica aerogels makes them impractical for structural applications although it has been created for over 70 years. Making silica aerogels mechanically robust is critical for promoting their applications.

Until now, some new methods including cross-linking the skeletal structure of silica aerogels with organic cross-linkers, incorporating fibers into the aerogels' matrix, or employing trifunctional silicon compounds as precursors have improves mechanical strength and flexibility of silica aerogels. These methods, however, also bring in some disadvantages such as, increased density, decreased surface area, and reduction in thermal insulation ability. Hence, how to enhance the mechanical properties of silica aerogels while retaining their low thermal conductivity become increasingly more important to promote their applications, especially for thermal insulations.

3. Investigations of the Sol-Gel Parameters on the Physical Properties of Silica Aerogels

3.1 Introduction

Silica aerogels are mesoporous materials consisting of nanosized building cells with numerous remarkable properties, such as low densities (0.003-0.35 g/cm^3), high surface area (600-1000 m^2/g), high porosity (>90%), excellent sound damping and low thermal conductivities (~0.015W/mK)[3]. Various applications based on the properties of interest have been documented in numerous review papers [8-13]. Among the applications, the most attractive and promising application for silica aerogels is thermal insulation. However, the fragility of silica aerogels makes them impractical for structural applications, though silica aerogels have been discovered for over 70 years. Thus, making silica aerogels mechanically robust by improving their ductility is critical for promoting their applications.

Previous investigations have shown that the synthesis conditions (for example, the ratio of H_2O: Si, the type and concentration of catalyst, and solvent, temperature, etc.) during sol-gel process strongly affect the resulting structure of gel network and the physical properties of silica aerogels[14,15]. Those sol-gel parameters also determine the kinetics and mechanism of sol-gel chemical reactions, as well as the generation and aggregation of the particles or clusters, involving in formations of various gel 3-D structures. Currently, silica aerogels are produced from sol-gel processes based on either 1-step acid or basic method, or 2-step acid-basic method. Usually, polymeric-like network with small pores is formed under acid conditions owing to the entanglement of less branched long chains, while under basic conditions, highly branched polymeric structure with larger pores is formed from the aggregation of larger clusters. Since the connectivity of gel network resulting from various sol-gel processing largely determines the mechanical properties of silica aerogels, many researchers have been working on increasing the particle or clusters' connectivity of silica aerogels through

structure modifications such as addition of polymer crosslinkers and fibers to modify the mechanical properties of aerogels (see Section 2.1.3).

In our research, we present a novel modified sol-gel process, a 3-step method. By using the method, silica aerogels with improved ductility and extremely low thermal conductivities have been successfully developed. Various advanced characterizations including BET and SEM are performed to study the effects of sol-gel processing parameters on the structural and physical properties of silica aerogels.

3.2 Experimental

3.2.1 Preparation methods of silica aerogels

3.2.1.1 Materials

Tetraethyl orthosilicate (TEOS, $\geqslant$ 98.0% (GC)), n-hexane(anhydrous), and ammonia standard solution(2.0 M in ethanol) were purchased from Sigma-Aldrich and used as received. Deionized water was obtained from Ricca Chemical Company. Anhydrous ethanol (ACS/USP grade) was from Pharmoco-Aaper Inc. Other materials were: hydrochloric acid (0.05 M) from ARISTAR and ammonium fluoride (1 M) from Acros Organics, both in the form of deionized water solutions. For supercritical drying, liquid carbon dioxide tank with siphon tube was purchased and used as received from Airgas Inc.

3.2.1.2 Procedure

All the silica aerogels were prepared in four steps: (i) hydrolysis of TEOS, (ii) condensation and gelation, (iii) aging and washing, and (iv) low temperature supercritical CO_2 drying.

In order to study the effects of catalysts and solvent on the structure and physical properties of the silica aerogels, two different synthesis routes were employed, 2-step method and 3-step method. In the first set of experiments, silica aerogels (sample

N-1-0-0 and F-1-0-0) were prepared through a 2-step method sol-gel process. In the first step, the precursor solution was placed for hydrolysis with substoichiometric water under acid condition for 1.5h with the molar ratios of starting materials TEOS: EtOH: H_2O: H^+ were kept at 1: 3: 1: 7 10^{-4}. During the second step, additional EtOH and water were added to increase the ratio to TEOS: EtOH: H_2O = 1: 8: 4. After that, 1ml ammonia solution (2M) or 1ml ammonium fluoride (1M) was added to induce condensation and gelation for sample N-1-0-0 or F-1-0-0 respectively. In the second set of experiments, silica aerogels (sample F, N, 0.01-8E-0-0, F, N, 0.01-12E-0-0, F, N, 0.01-16E-0-0, and F, N, 0.01-20E-0-0) were prepared through a 3-step method sol-gel process. The first step is the same as described in the first set of experiments. In the second step, additional EtOH, water and ammonia solution were added to increase the ratios to TEOS: EtOH: H_2O: $NH_3 \cdot H_2O$ = 1: 8 (12, 16, or 20): 4: 2 10^{-3}, while stirring for 0.5h. In the third step, 1ml ammonium fluoride (1M) was added as gelation agent and sol solutions were poured into molds before gelation point. In the third set of experiments, silica aerogels (sample F, N, 0.002-16E-0-0, F, N, 0.004-16E-0-0, F, N, 0.006-16E-0-0, F, N, 0.008-16E-0-0, and F, N, 0.01-16E-0-0) were prepared also through a 3-step method sol-gel process. In this experiment set, the first step is the same as described in the previous, and during the second step, additional EtOH, water and ammonia solution were added to increase the ratio TEOS : EtOH : H_2O : $NH_3 \cdot H_2O$ = 1 : 16 : 4 : 2 10^{-3}, with stirring for 0.5h. For the third step, 1ml ammonium fluoride 0.2M(0.4M, 0.6M, 0.8M, or 1M, respectively) was added as gelation agent and sol solutions were poured into molds before gelation point. All the wet gels obtained were aged for three days under ethanol before washing. Then, the wet gels were washed three times, 24h for each, prior to supercritical drying.

A homebuilt system (see Figure 3.2.1) was employed for supercritical drying of wet gels. Before drying, the wet gels were placed into an autoclave ($100cm^3$) in an ethanol bath. The autoclave was then sealed and liquid carbon dioxide at 4 ^{0}C was pumped in at a rate of 20 psi/min until the pressure reached to 1400psi. At the same time, the

autoclave was heated up to 40^0C (i.e. above the critical point of CO_2, Pc= 1070 psi, Tc=31.1^0C). After reaching 40^0C, the pressure was kept constant at 1400psi and the outlet valve was opened, so that the solvent extracted by supercritical CO_2 was able to flow out with a rate of 3ml/min. 700ml of liquid CO_2 was needed to complete the extraction process at this stage. Finally, the system was slowly depressurized at a rate of -2psi/min. When ambient pressure was reached, the system was cooled down to the room temperature. Silica aerogels were thus obtained and ready for further characterizations.

3.2.2 Methods of Characterizations

3.2.2.1 Density and Porosity

Bulk density ρ of silica aerogels was defined as the ratio of weight to volume, where the weight was measured with a microbalance with an accuaracy down to 10^{-5} grams, and the volume of silica aerogels was measured geometrically. Volume shrinkage, $V_{shrinkage}$ of the silica aerogels was calculated from the volumes of gels before (V_{wet}) and after (V_{dried}) supercritical drying. Porosity was determined as follows from the bulk density ρ, assuming a skeletal silica density ρ_{SiO_2} of 2.2 g/cm^3.

$$V_{Shrinkage}\% = (1 - V_{dried} / V_{wet}) \times 100 \quad (3.2.1)$$

$$Porosity = (1 - \rho / \rho_{SiO_2}) \times 100 \quad (3.2.2)$$

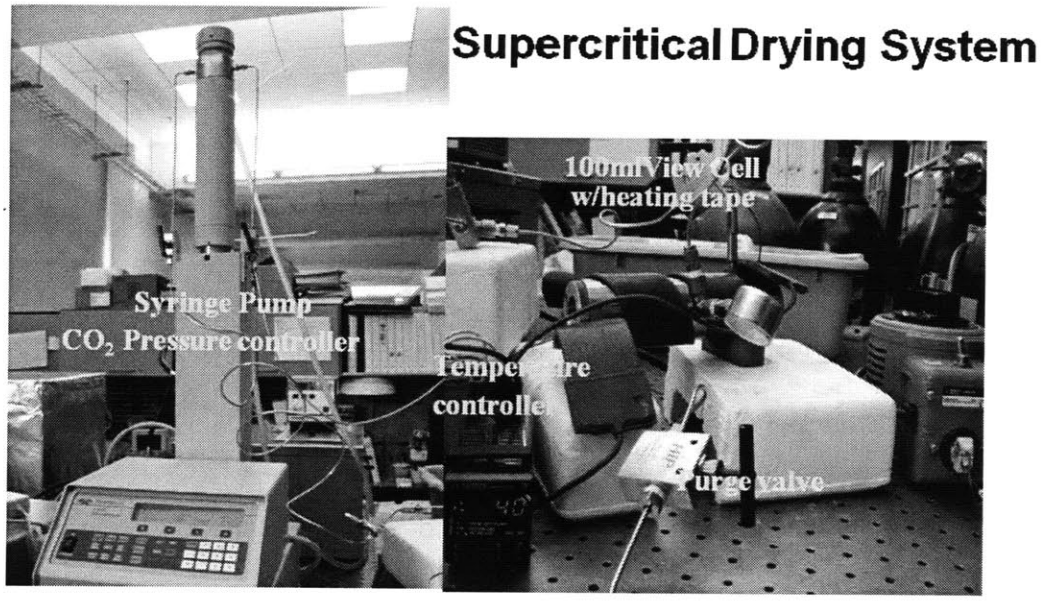

Figure 3.2.1 Homebuilt Supercritical Drying System

3.2.2.2 Structural Feature

Nitrogen adsorption/desorption measurements (BET method) were performed to obtain BET surface area, mesopore volume, and pore size distribution with an ASAP 2020 instrument (Micromeritics, USA). Before analysis, samples were degassed under vacuum at 150^0C for at least 2h. An FESEM-6700 (JEOL, Japan) was employed on gold-coated aerogels samples to observe the network morphology.

3.2.2.3 Mechanical Properties

The flexural modulus (E) and the yield strength (σ) of the silica aerogels samples were measured by a three point bending technique using Instron 8848 Micro Tester with a 10N loading cell. The precision of the measurement was 0.01N. The measurements were preformed using cylindrical shaped samples with a diameter of about 0.8cm and a span of 3 cm. The loading speed was 1mm/min. Figure 3.2.2 is a schematic illustration of the experimental setup.

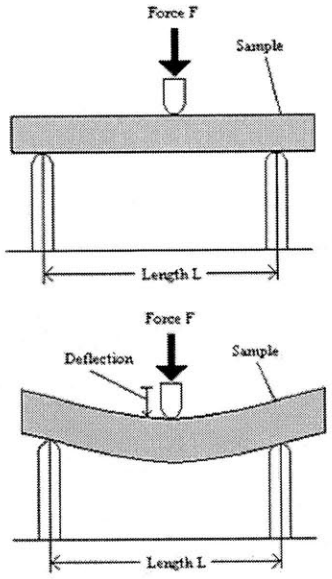

Figure 3.2.2 Schematic illustration of three-point-bending measurement

$$\sigma = \frac{F_{\max} L}{\pi r^3} \tag{3.2.3}$$

$$E = \frac{SL^3}{12\pi r^4} \tag{3.2.4}$$

Where, σ= yield strength, E = flexural modulus, S = slope of the stress-strain curve, L = span of the two supports, r = radius of the sample.

3.2.2.4 Thermal Conductivity Measurements

Thermal conductivity measurements of silica aerogels were conducted using the transient hot wire method developed by Nagasaka and Nagashima [86]. Resistance technique was used in our experimental measurements, where the temperature of the wire was measured by the change in resistance caused by the heating up of the hot wire, and the mean temperature rise of the wire was calculated along its particular length,

eliminating the influence of local non-homogenous of measured samples [88]. For deducing the thermal conductivity of the samples, a mathematical model of transient hot wire method was utilized. The model involves several assumptions: (i) infinite long hot wire surrounded by infinite materials whose thermal conductivity is to be measured; (ii) the wire is a perfect thermal conductor with uniform temperature; (iii) Only radial heat loss through the measured medium around the wire occurs. The thermal conductivity of the silica aerogels was then calculated from the temperature history using a simplified formula as follows:

$$\theta - \theta_0 = \left(\frac{q}{4\pi k}\right)\left[-0.5772 + \ln\left(\frac{4at}{r^2}\right)\right] \tag{3.2.5}$$

Where, θ = hotwire temperature (θ_0 = initial temperature), q = power dissipated per meter hot wire (W/m), r = hotwire radius, k= thermal conductivity, a = thermal diffusivity. The condition of $r^2/4at \ll 1$ should be fulfilled for the validation of the formula. Thermal conductivity, k is determined from the slope of the temperature rise history, K as follows:

$$K = \frac{d\theta}{d(\ln t)} \tag{3.2.6}$$

Then, the linear region of temperature rise evolution $\Delta\theta$ vs. natural logarithm of the time ln(t) is applied to obtain thermal conductivity:

$$k = \frac{q}{4\pi K} \tag{3.2.7}$$

Nanofluid Thermal Conductivity Measurement System (developed by NanoEngineering Group at MIT) was employed for thermal conductivity measurements of silica aerogels. Figure 3.2.3 shows the schematic diagram of the data acquisition system. The history of hotwire temperature was measured by a Wheatstone Bridge with

two arms of the bridge consist of two precision resistors and the other two arms of the bridge consist of the sample with built-in hotwire and a potentiometer. The voltage imbalance across the bridge as a function time was then recorded by a GPIB Board.
Unlike the measurements of thermal conductivity measurements for liquid, the measurements for solid materials present a great challenge, as it is difficult to realize good thermal contact between the hotwire and the measuring sample (i.e. silica aerogels). To overcome the challenge, an in-situ hotwire method was developed to prepare the silica aerogels samples with hotwire embedded in. First, a bare platinum hotwire (25 μ m in diameter) was suspended in the sol solution prior to gelation point. Then, after gelation, aging, and washing, wet gel with built-in hotwire was maintained intact for supercritical CO_2 drying. Dried gel was used for thermal conductivity measurement (see Figure 3.2.4). Since the hotwire was built into the aerogel sample from liquid phase, good thermal contact between the wire and sample were easily realized. as the process also ensures no thin air surrounding the wire. Furthermore, compared to previous high pressure cell method with external loading applied to ensure thermal contact [89], our in-situ hotwire built method better protects the behavior of internal structure of silica aerogels.

For measuring the thermal conductivity, silica aerogel samples with built-in hotwire were first connected into the system. The resistances of the hotwire were measured with a Digital Multimeters (DMM's) using the four-wire method. The potentiometer was then adjusted to balance the bridge. After the bridge was initially balanced, a constant current of 28 mA (40mA for thermal conductivity measurements of ethanol and hexane) was applied to the bridge, and the voltage imbalance across the bridge was recorded as a function of time. The duration of data acquisition was kept for a second. Finally, signal analysis was performed to convert the bridge output signal to the thermal conductivity of the measured sample. To secure the reliability of the method, measurements of anhydrous ethanol and n-hexane with known thermal conductivity values were performed. The measured values were all within 1.5% of literature ones

(see Table 3.2.1) [87]. The uncertainty shown in the measured thermal conductivity was obtained from the standard deviation of six data points.

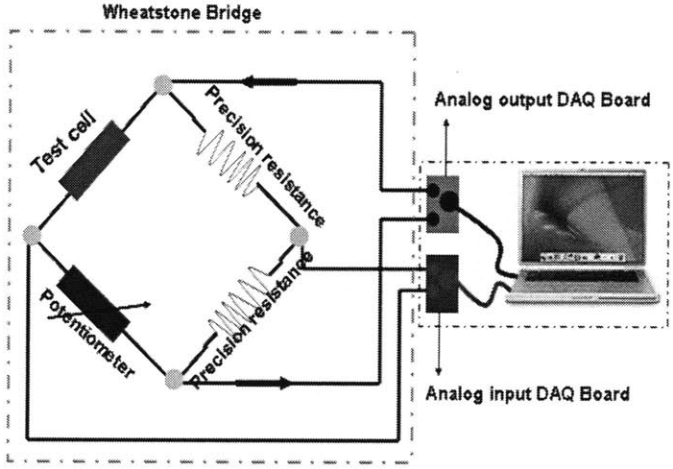

Figure 3.2.3 Schematic diagram of the data acquisition system for thermal conductivity measurements

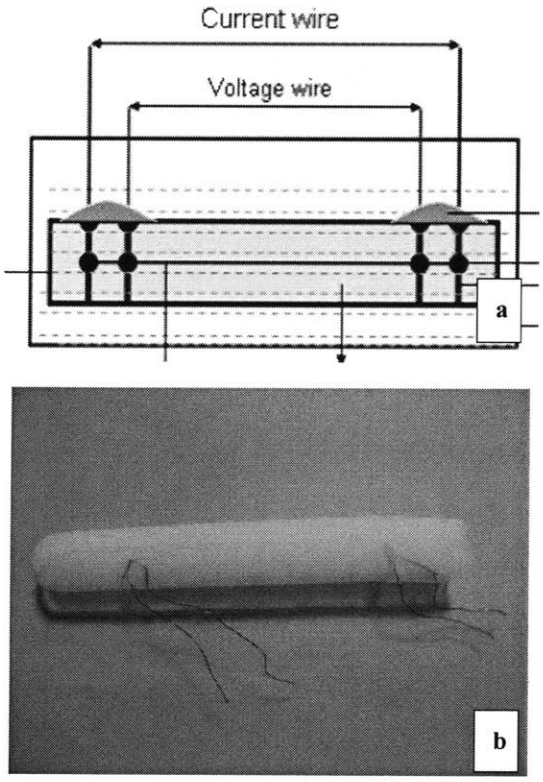

Figure 3.2.4 Schematic diagram(a) and actual photo(b) for the sample cell

Table 3.2.1 Measured Thermal Conductivity vs. Literature Values

Sample	Literature Value (W/mK)	Measured Value (W/mK)	Error (%)
Ethanol(anhydrous) (20^0C)	0.168	0.170 ± 0.002(±1σ)	1.2%
n-Hexane (20^0C)	0.126	0.125 ± 0.002(±1σ)	-0.8%

* Error = $[(k_{measured} - k_{literature})/k_{literature}] \times 100$

The effects of hotwire length on the thermal conductivity measurements were investigated by measuring the same sample using different lengths of hotwire. We first measured a fumed silica sample (with reported k=20.5mW/mK) from NIST and a silica aerogel sample (F,N,0.01-20E-0-0), respectively. The temperature rises were all less than 6^0C with an applied constant current of 28 mA (see figure 3.2.5). Evidently, with the same current, the temperature rises in silica aerogel samples are all much higher, which is mainly contributed to the lower thermal conductivity of silica aerogel than the NIST sample. Based on the two sets of measurements (see Figure 3.2.7), we observed that, as the length of hotwire increased, the measured values became independent of the length, and a length of 6.5cm is sufficient. Thus hotwires with a length of ~6.5cm were used for thermal conductivity measurements on all silica aerogels samples.

It has been noticed that the measured value (22.3 mW/mK) of fumed silica was about 10% higher than the standard value (20.5 mW/mK). We contribute the higher measured value to the end effects. During each measurement, the ends of the Pt wire are at a lower temperature than the center because the copper wires (254 μm in diameter) to which the Pt wire is soldered, have smaller resistance than surrounding measured materials, and a heat loss for the hotwire exists(see Figure 3.2.6). Thus, from Eq. 3.2.6 and Eq. 3.2.7, it can be seen that the end effects result in higher measured values than the true values.

$$k_{measure} = \frac{q}{4\pi \frac{d\theta}{d(\ln t)}} \qquad k_{true} = \frac{q - q_{loss}}{4\pi \frac{d\theta}{d(\ln t)}} \tag{3.2.6}$$

$$\frac{k_{measure}}{k_{true}} = \frac{q}{q - q_{loss}} \tag{3.2.7}$$

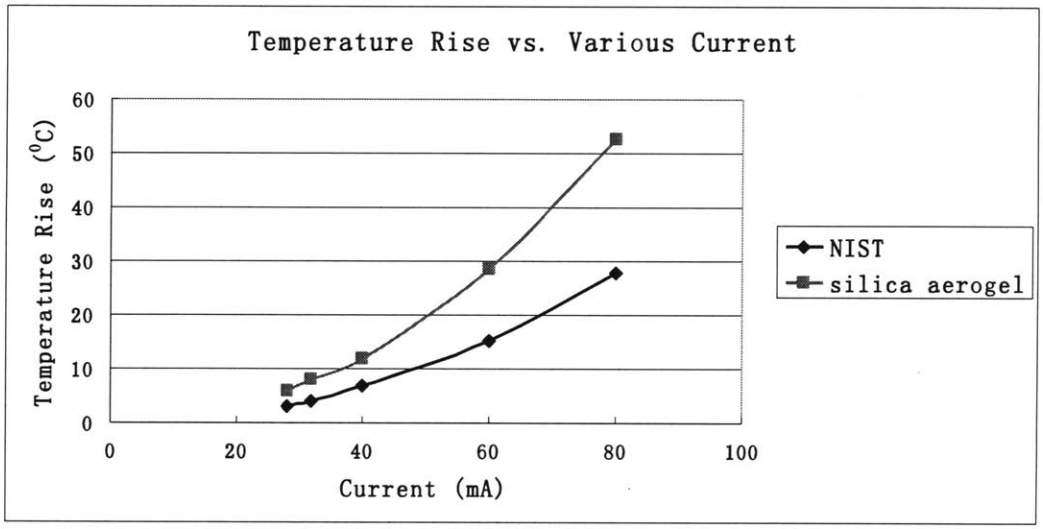

Figure 3.2.5 Thermal conductivity measurements under various constant current.
For each measurement, 28A, 32mA, 40mA, 60mA or 80mA was applied for duration of 1s.

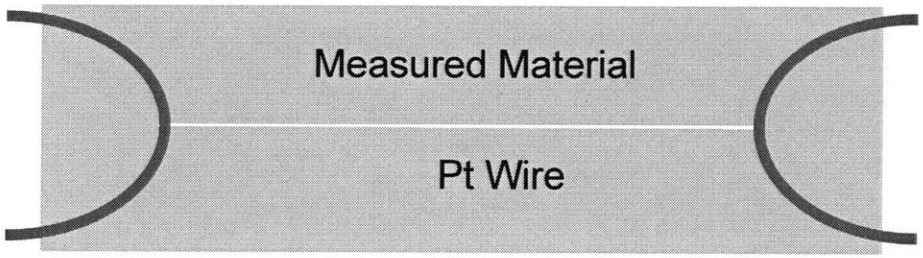

Figure 3.2.6 Schematic diagram of Pt hotwire and copper wire embedded within a measured material

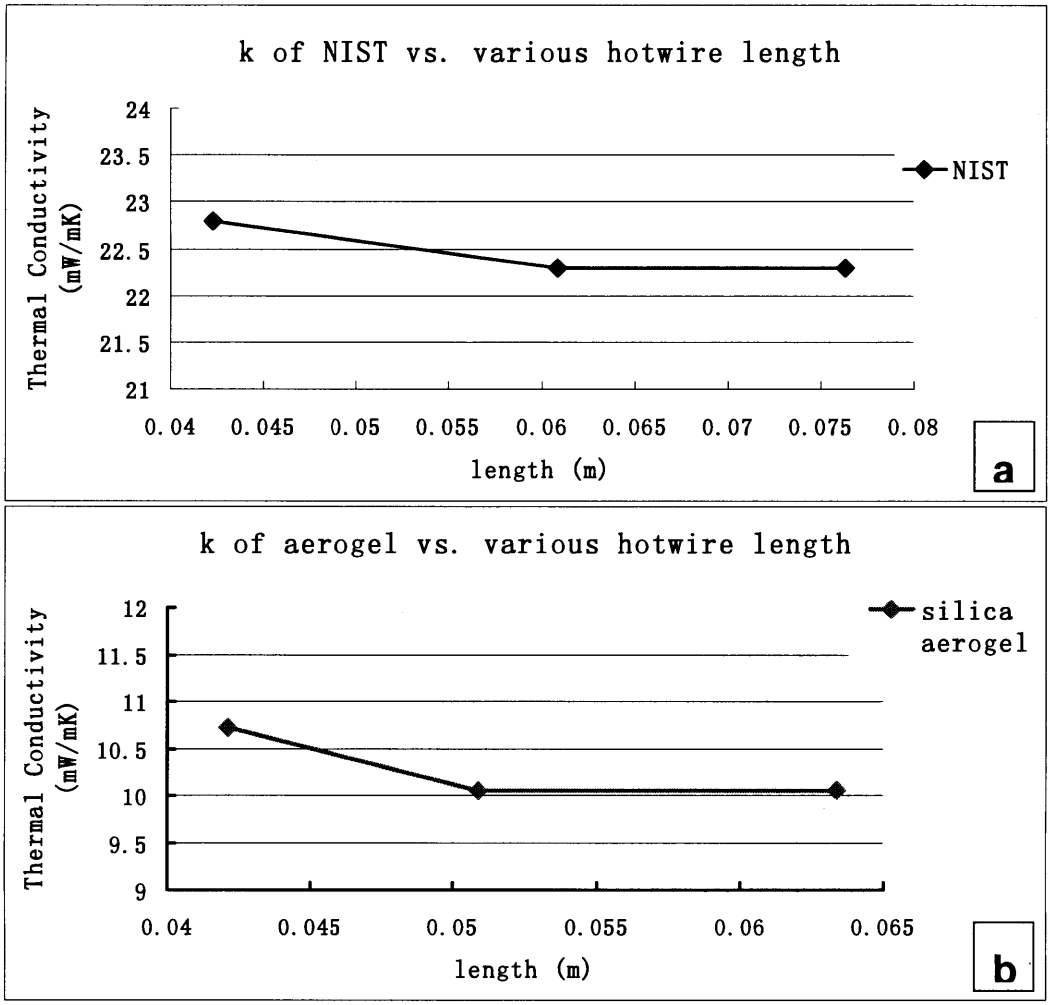

Figure 3.2.7 Effects of hotwire length: fused silica (a) and silica aerogel (b)

3.3 Results and Discussions

3.3.1 Effects of Different Catalysts

Two different synthesis routes have been developed, a 2-step method (sample N-1-0-0 and sample F-1-0-0) and a 3-step method (sample F, N, 0.01-8E-0-0). The first steps of these two synthesis routes are performed under the same reaction condition. Table 3.3.1 shows the properties of silica aerogels prepared. During the second step of 2-step method, which is mainly for condensation and gelation, sample N-1-0-0 is catalyzed by addition of 1M $NH_3 \cdot H_2O$ solution, while, sample F-1-0-0 is catalyzed by addition of 1M NH_4F solution. For the 3-step synthesis route, sample F, N, 0.01-8E-0-0 is prepared by adding $NH_3 \cdot H_2O$ during the second step for condensation, following with addition of NH_4F during the third step to induce gelation. Compared to the mechanical properties of those three samples, F-1-0-0 and F, N. 0.01-8E-0-0 have a higher yield strength and lower flexural modulus than N-1-0-0, leading to better ductility. However, the standard deviation of flexural modulus of F-1-0-0 is much larger than that of F, N, 0.01-8E-0-0, meaning a poor integrity of mechanical behaviors. Thus, the 3-step sol-gel process using a combination of $NH_3 \cdot H_2O$ and NH_4F to allows separate control for condensation and gelation, produces silica aerogels with better ductility and mechanical integrity. In addition, from our transient hotwire measurements, thermal conductivity of sample N-1-0-0 is higher than that of sample F-1-0-0 and F, N, 0.01-8E-0-0, yet, all of them are much lower than air (25mW/mK).

Table 3.3.1 Properties of Silica Aerogels prepared from 2-step method and 3-step method

Sample	Yield Strength(kPa)	Flexural Modulus(MPa)	Bulk Density(g/cm^3)	Porosity (%)	Thermal Conductivity (mW/m.K)
N-1-0-0	47.4+/-5.7	1.44+/-0.08	0.146+/-0.003	93.4	11.08 +/- 0.03
F-1-0-0	69.2+/-19.2	1.49+/-0.32	0.128+/-0.002	94.2	9.09 +/- 0.02
F,N,0.01-8E-0-0	73.3+/-19.3	1.34+/-0.03	0.131+/-0.001	94.0	9.32 +/- 0.02

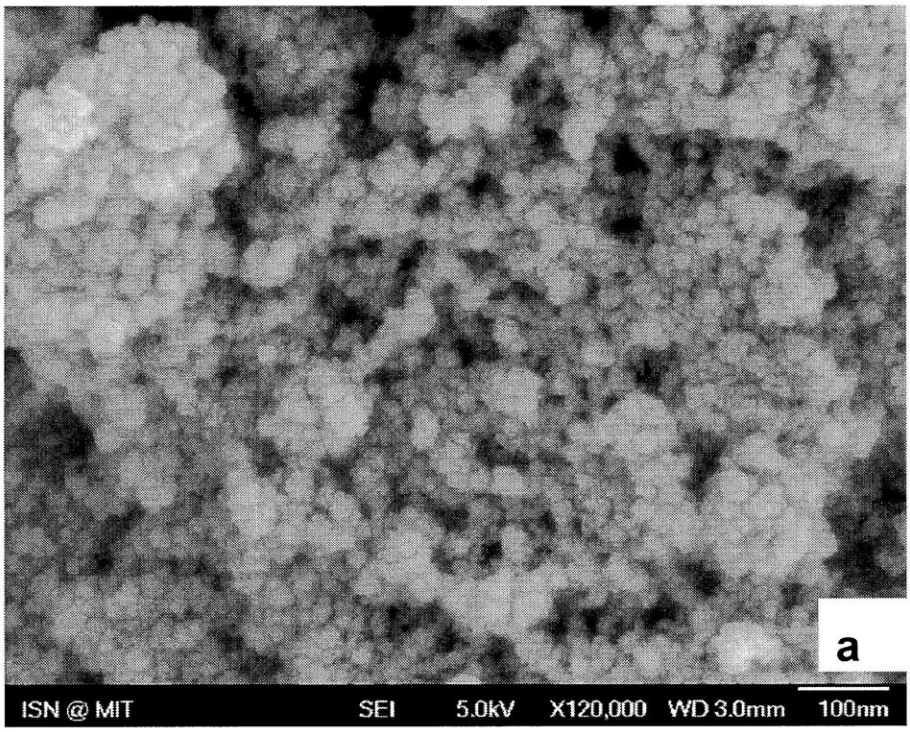
a
ISN @ MIT
SEI
5.0kV
X120,000
WD 3.0mm
100nm

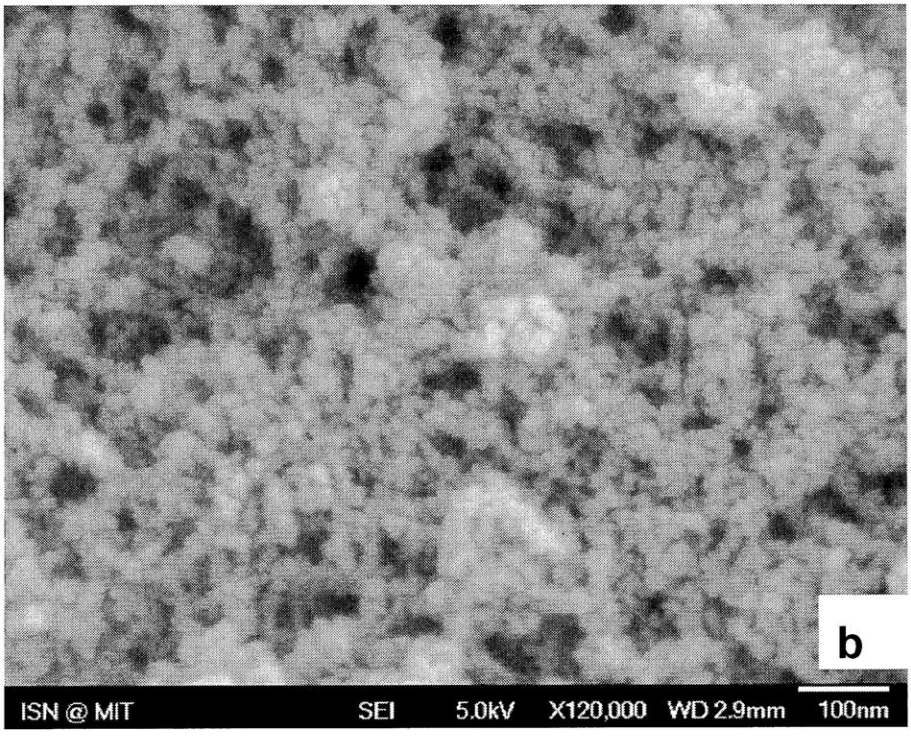
b
ISN @ MIT
SEI
5.0kV
X120,000
WD 2.9mm
100nm

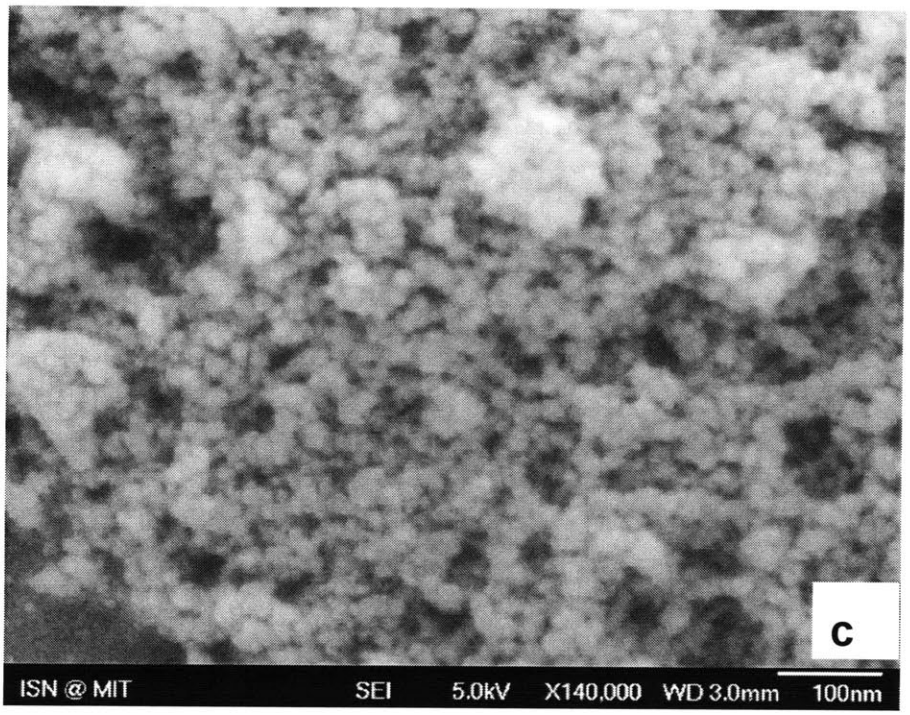

Figure 3.3.1 SEM images of silica aerogels samples: (a) N-1-0-0 and (b) F-1-0-0 were prepared from 2-step method, and (c) F, N, 0.01-8E-0-0 was prepared from 3-step method

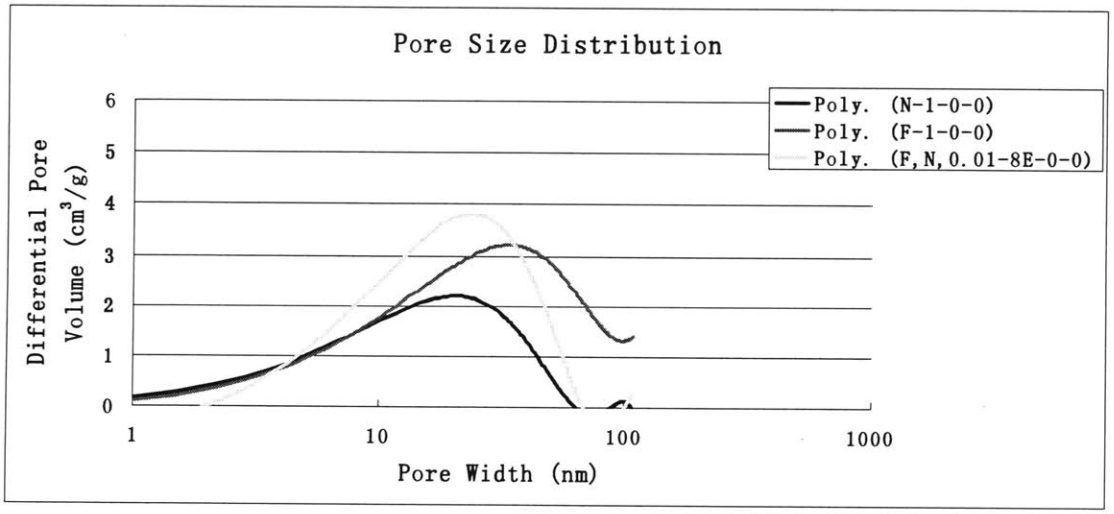

Figure 3.3.2 Pore size distribution of silica aerogels

Figure 3.3.1 shows a couple of high magnification SEM images of silica aerogels prepared from the 2-step method and 3-step method., Their difference in structure feature can be clearly observed. It has been well known that the primary particle diameters of silica aerogels are around 2~5nm [3], which are very difficult to be seen under SEM. One yet can clearly distinguish the secondary clusters in all the SEM images. In Figure 3.3.1(a), we observe condensed gel networks consisting of less pore volume and secondary clusters with high consolidation. While, in Figure 3.3.1(b), less condensed gel networks with highly branched polymeric secondary clusters in diverse sizes and larger pores are observed. In Figure 3.3.1(c), we observe less condensed gel networks composed of highly branched polymeric secondary clusters with more uniform size as well as larger pores. Furthermore, BET pore size distributions (see Figure 3.3.2) provide us more in sight information about the porous structure. More large pores and increasing in pore volume are presented in sample F-1-0-0 and F, N, 0.01-8E-0-0, which favor the less condensed gel networks. And the much broader pore size distribution of sample F-1-0-0 confirm the diverse in clusters size, while a narrow pore size distribution of sample F, N, 0.01-8E-0-0 corresponds to more uniform clusters size.

We thus speculate that the improved ductility of NH_4F catalyzed samples benefit from the highly branched secondary clusters and increased pore volumes. This makes sense, since connectivity between clusters increases as clusters become more branched and larger pores give more space for the possible motion of clusters in response to external loading. If the gel network is composed of condensed secondary clusters with high consolidation and fewer pores such as in sample N-1-0-0, a relatively rigid mechanical behavior for the aerogel is anticipated. The enhanced solid conduction due to the consolidation of secondary clusters also contributes to the higher thermal conductivity of sample N-1-0-0.

We also speculate that the effects of different catalysts on the structural and the physical properties of silica aerogels come from the different condensation and gelation

rate. For sample N-1-0-0, during the second step of preparation, only $NH_3 \bullet H_2O$ is involved for condensation and gelation, and it takes about 50 minutes before gelation occurs. In comparison, gelation occurs in less than 2 minutes with the addition of NH_4F for the other two samples. Since pore structure of gel networks depends on both of the clusters size and clusters packing geometry, a longer gelation produces a more highly condensed gel structure, leading to a higher flexural modulus. Not surprisingly, sample N-1-0-0 appears to be more rigid than the other two samples.

The significant reduction in gelation time by using NH_4F is due to the unique catalytic effects on the rate of condensation reactions. The mechanism for F^- catalyzed condensations is mainly from the displacement of OH^- with F^-, causing localized attractions to surrounding silanol groups, thus promoting the condensations [45]. Furthermore, since F^- is more electron-withdrawing than OH^-, the replacement of F^- with OH^- causes reduction of electron density of Si, thereby facilitating nucleophilic attack from other OH^- groups. Therefore, the F^- could strongly promote the condensation reactions and crosslinking among clusters, leading to the formation of highly branched polymeric structure with large pores.

However, gel networks formed from simultaneous condensation and crosslinking of clusters produces silica aerogels with poor mechanical integrity. When condensation and gelation occur within such a short time, each reactive cluster reacts with surrounding clusters without any preference. Consequently, the formed gel networks consist of clusters with diverse sizes, and the mechanical integrity is poor. By using a 3-step method, the shortage has been successfully overcome. During the 3-step method, we utilize three different catalysts to perform separate controls of hydrolysis, condensation and gelation (see Figure 3.3.3). With the addition of HCl in the first step, the solution pH is 2~3. At this stage, hydrolysis reactions are active and small reactive silanol oligomers are formed. During the second step, a certain amount of $NH_3 \bullet H_2O$ is added, the sol solution pH increases up to 6~7, and condensation reactions become more active in the system. When condensation reactions occur in an environment with

pH between 6 ~ 7, silica clusters are preferentially growing through the addition of monomer to larger clusters rather than aggregation among larger clusters. Additionally, the solubility of silica is much higher in a solution with pH = 6 ~ 7 (Figure 2.1.7), and the smaller clusters (e.g. < 2nm) are even more soluble than larger clusters (e.g. 2~5nm). We speculate that these two effects facilitate the smaller cluster reduce to molecules which then combine with other cluster to form larger clusters, called primary clusters.

When NH_4F is added as inducing agent for gelation in the third step, the residue of the reduced silanol molecules or oligomers react with other to form small clusters, or attach to larger clusters to form branched polymeric clusters, called secondary particles. Meanwhile, cross-linking occurs between clusters. These three possible simultaneous processes contribute to formation of hierarchical structure for aerogels consisting of lots of small pore structures embedded in large pores. We speculate that in the hierarchical structure, some clusters with loose connectivity are easy to move, and the motions are accommodated by the large pore structure. Hence, the synthesized silica aerogels have improved ductility and better mechanical integrity.

In summary, the proposed 3-step method has separate controls for hydrolysis, condensation and gelation. The method can be used to tune the clusters growth and network formation during sol-gel process. The synthesized silica aerogels thus have a good quality in terms of low density; low thermal conductivity, better ductility and mechanical integrity.

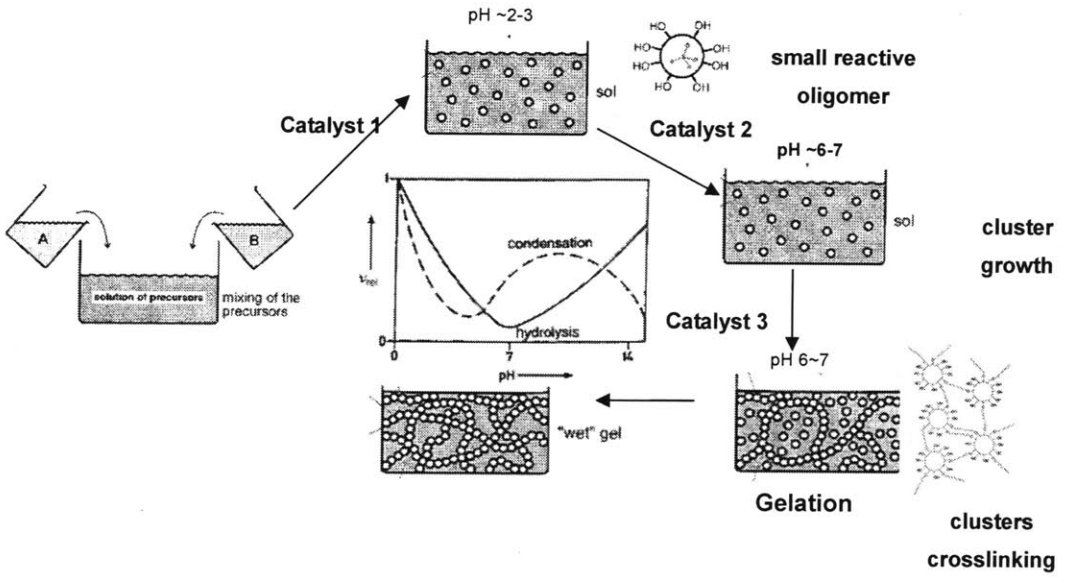

Figure 3.3.3 Schematic illustration of the 3-step method for sol-gel process, where, catalyst 1, 2, 3 represent HCl, $NH_3 \cdot H_2O$ and NH_4F, respectively

3.3.2 Effects of Solvent Concentration

In order to further investigate the effects of sol-gel processing parameters on the physical properties of silica aerogels, we prepared samples with various solvent concentrations and catalyst concentrations using the 3-step method.

First, by keeping all the other parameters at constant values, samples with molar ratios of EtOH : Si varying from 8 to 20 were prepared. Table 3.3.2 shows the physical properties of silica aerogels corresponding to different molar ratios of EtOH: Si. Accordingly, the number before E is the molar ratio of EtOH : Si.

From Table 3.3.2, it can be seen that the aerogel's density, yield strength, and flexural modulus all decrease with increasing molar ratios of EtOH : Si. Aerogels with densities lower than 0.01 g/cm^3 are obtained with the molar ratios of 16 and 20. However, the molar ratio of 20 gives a volume preserved shrinkage of 80.8%. A possible reason is that the prepared wet gels are sensitive to drying conditions and

couldn't withstand the drying stresses. Consequently, a higher volume shrink occurs after being dried. It looks like that wet gels prepared from molar ratio of 16 has more tolerance with drying conditions, so up to 91.2% in volume preserved shrinkage has been well retained. It is worthwhile to note that, the measured thermal conductivities of these aerogels are around 9~10 mW/m.K, much lower than previous reported silica aerogels' thermal conductivity of 15 mW/m.K [3].

It must be pointed out that, both the yield strength and the flexural modulus decreases with increasing solvent concentration. In order to better investigate the solvent effects on silica aerogel's mechanical properties especially the ductile, we introduce a new parameter, the reduction ratio. If we take the yield strength and flexural modulus of sample F,N,0.01-8E-0-0 with lowest solvent concentration as reference values, (P_0,E_0), and divide the yield strength and flexural modulus of other samples(P,E) by the corresponding reference value respectively, we can obtain the reduction ratios (P/P_0, E/E_0). Figure 3.3.4 shows the reduction ratios in both yield strength and flexural modulus versus molar ratios of EtOH: Si. If the reduction ratio of yield strength is higher than that of flexural modulus, we believe that the resulting aerogel has improved elastic properties (ductility) than the reference sample. From the plots, samples with molar ratios of EtOH: Si =16 and 20 have improved ductility than the reference sample. The larger difference between reduction ratios (P/P_0, E/E_0) is, the better ductility of silica aerogels will be. Thus, increasing the solvent concentration improves the silica aerogels' ductility.

Table 3.3.2 Properties of silica aerogels prepared from different molar ratios of EtOH: Si

Sample	Yield Strength (kPa)	Flexural Modulus (MPa)	Bulk Density (g/cm^3)	Porosity (%)	Volume Preserved Shrinkage (%)	Thermal Conductivity (mW/m.K)
F,N,0.01-8E-0-0	73.3+/-19.3	1.34+/-0.03	0.131+/-0.001	94.0	95.1	9.32 +/- 0.02
F,N,0.01-12E-0-0	32.7+/-11.8	0.64+/-0.01	0.106+/-0.002	95.1	94.2	9.28 +/- 0.06
F,N,0.01-16E-0-0	23.8+/-4.3	0.39+/-0.03	0.091+/-0.001	95.8	91.2	10.01 +/- 0.02
F,N,0.01-20E-0-0	22.4+/-4.0	0.33+/-0.03	0.087+/-0.001	96.0	80.8	10.05 +/- 0.04

* Volume preserved shrinkage is calculated from the sample size after supercritical drying divided by the sample size before drying.

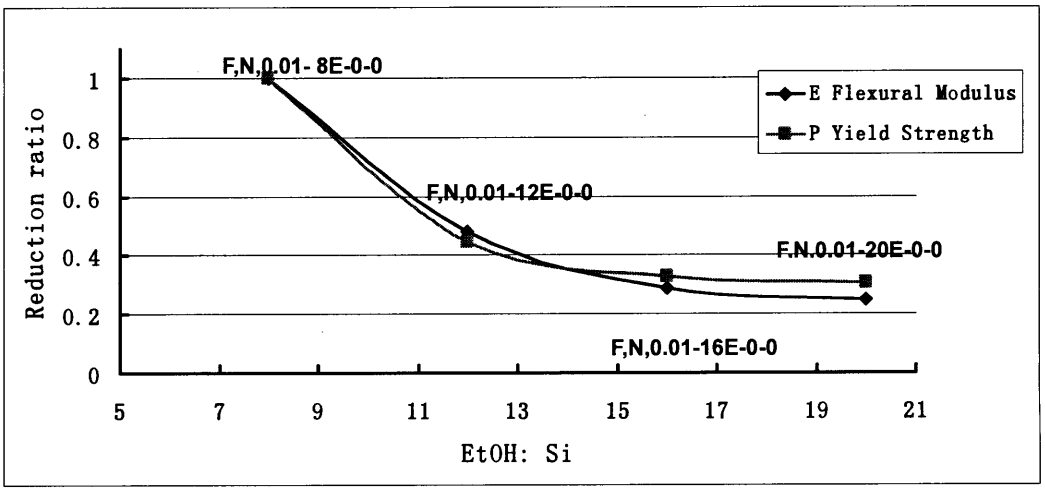

Figure 3.3.4 Reduction ratios in both yield strength and flexural modulus vs. molar ratios of EtOH : Si.

Figure 3.3.5 shows some high magnification SEM images of silica aerogels prepared with different solvent concentrations. It can be seen that all the four samples present networks composed of highly branched secondary clusters. The difference between these four samples is their porous feature. With increasing solvent concentration, the densities of the arerogels decrease. This is also consistent with the aerogel structure. From the images, it can be seen that the connectivity between clusters

become looser, and larger pores (>70nm) are presented. The BET pore size distributions further confirm the observations (Figure 3.3.6). With increasing solvent concentrations, the aerogels have more larger pores (diameter >70nm). All these four samples have, a broad pores size distribution.(ranging from several nanometers up to 100nm).

Based on the above observations, we conclude that increasing solvent concentration results in gel networks that have a looser connectivity and an increased pore volume from larger pores. The loose connectivity could contribute to the reduction in both yield strength and flexural modulus; nevertheless, increased larger pores' volume could further reduce the flexural modulus, because larger pores can provide more space for the movements of clusters in response to external loading. Thus we observe improved ductility in the prepared silica aerogels samples as the solvent concentration increases. From thermal conductivity measurements, a small increase in the thermal conductivities of samples with molar ratios of EtOH: Si at 16 and 20 has been observed, which is due to the increasing pore volume from larger pores (>70nm). A larger volume fraction of large pores lead to increased gas heat conduction resulting in higher total thermal conductivity for the aerogel.

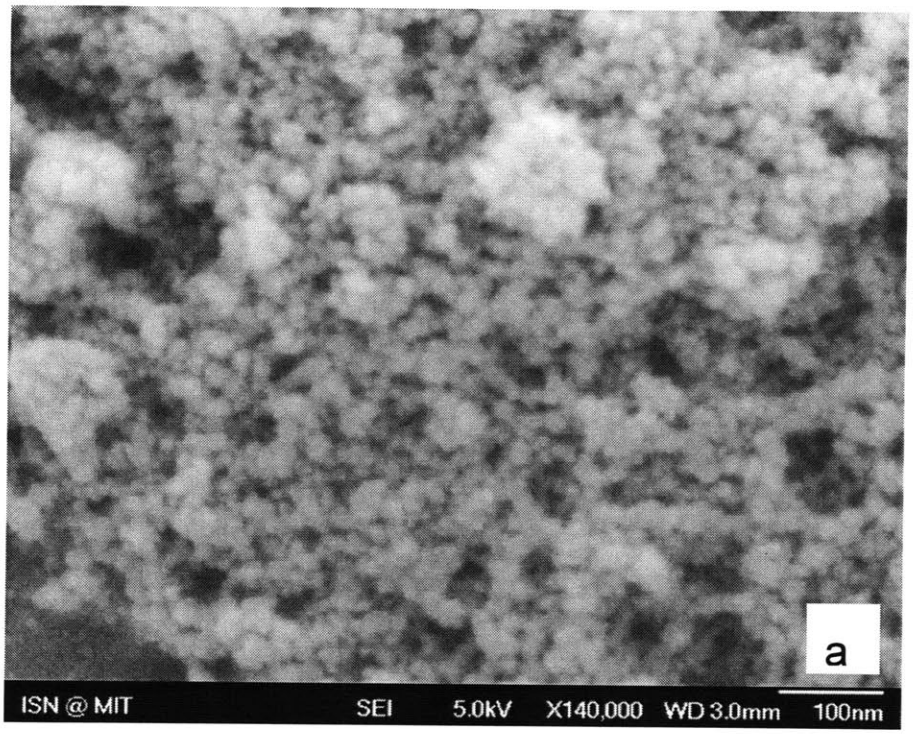
a
ISN @ MIT
SEI
5.0kV
X140,000
WD 3.0mm
100nm

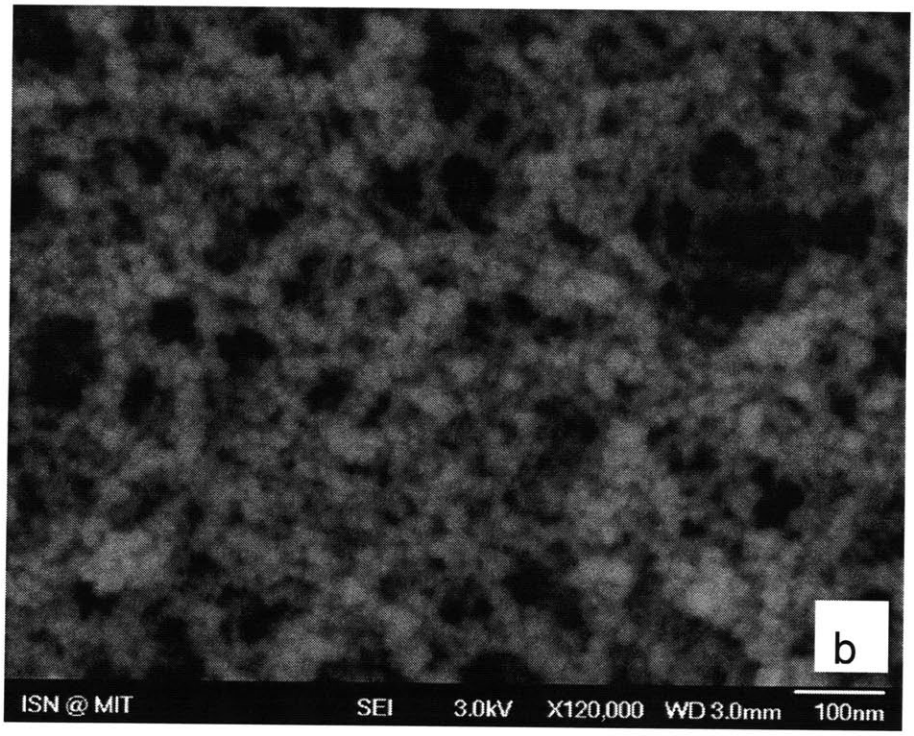
b
ISN @ MIT
SEI
3.0kV
X120,000
WD 3.0mm
100nm

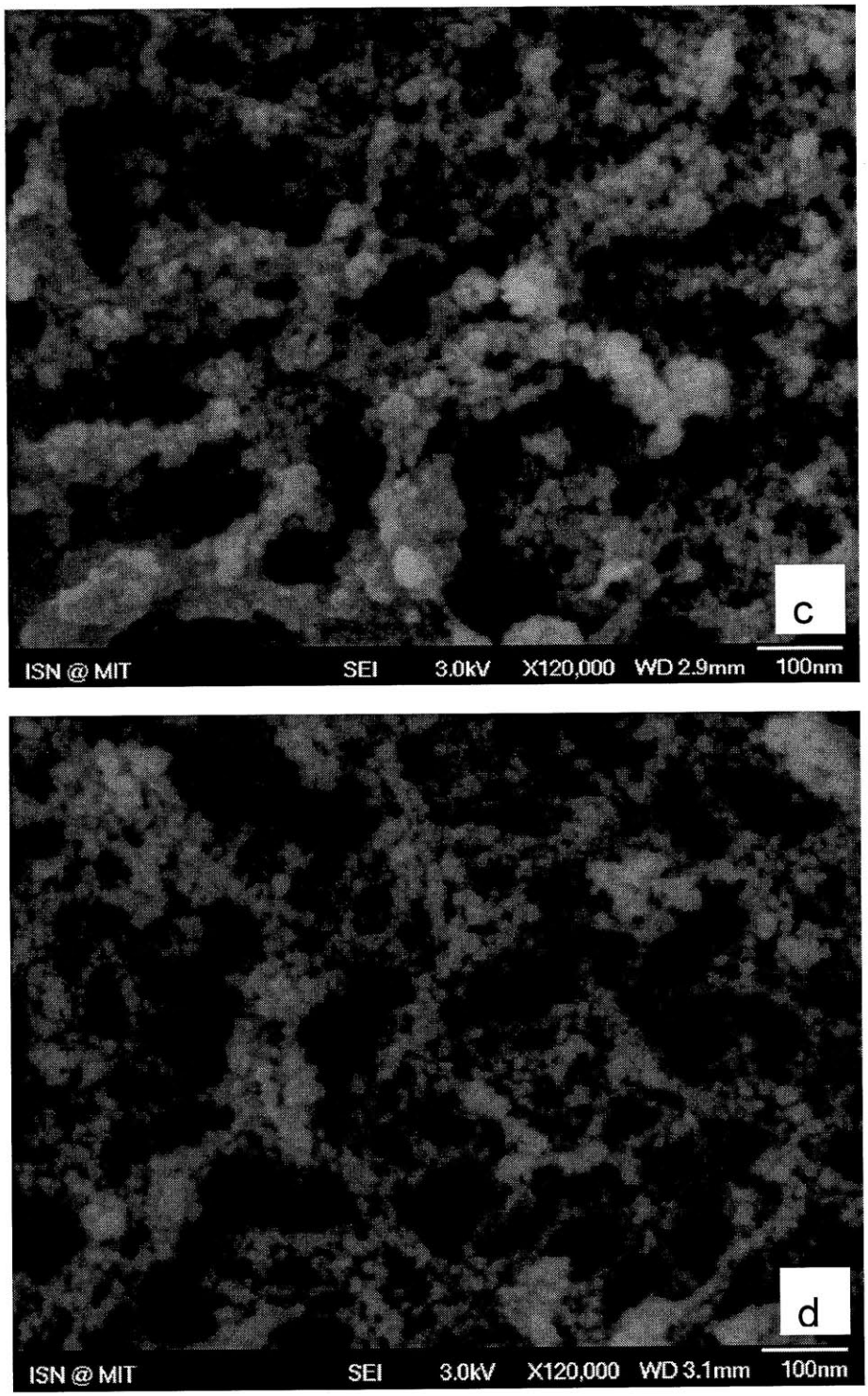

Figure 3.3.5 SEM images of silica aerogels samples prepared with various solvent concentration: (a) F,N,0.01-8E-0-0, (b) F,N,0.01-12E-0-0, (c) F,N,0.01-16E-0-0, (d) F,N,0.01-20E-0-0.

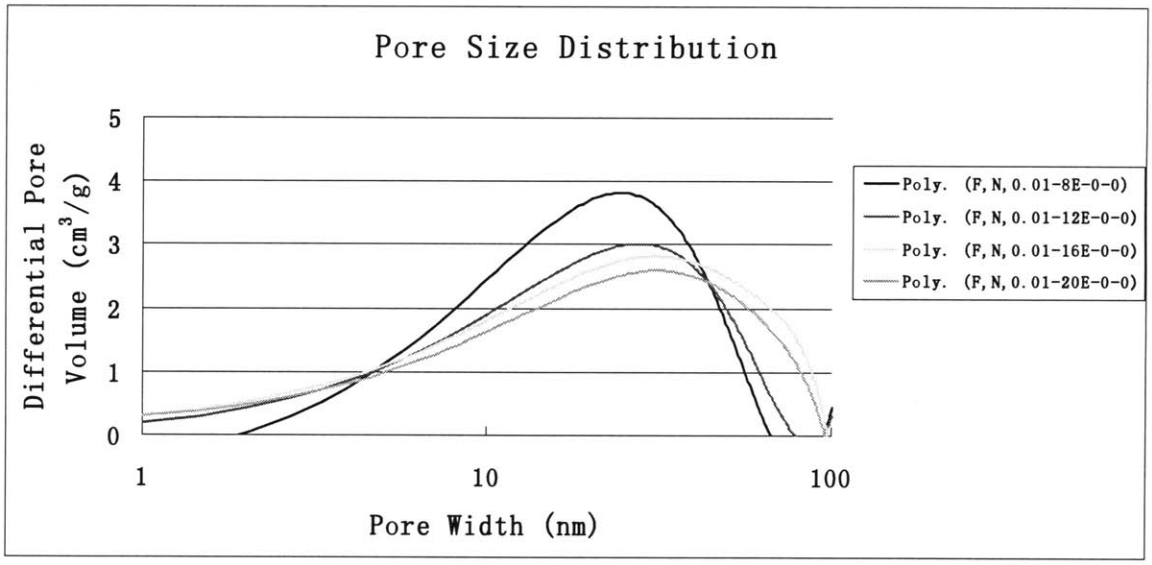

Figure 3.3.6 Pore size distribution of silica aerogels with various solvent concentrations

We speculate that one of the effect of solvent concentration on both of the yield strength and flexural modulus comes from its impact on condensation consisting of three possible pathways: 1) Increases in solvent concentration can decrease the concentration of hydrolyzed silanol clusters in the solution and increase the spacing between the reacting species, which in turn decrease the condensation rate and result in a longer gelation time; 2) In ethanol environment, under base-catalyzed condensation, hydrogen bonding is more likely formed between the ethanol molecules and deprotonated silanols, resulting in further decreased condensation rate; 3) The ethanol molecules are prone to form hydrogen bonding with OH^-, which enable OH^- to be even weaker nucleophile, and reduce the condensation rate. This speculation is also supported by the observed longer gelation time when solvent concentrations increases.

When the condensation rate is reduced, there will be a lot of un-reacted -OH groups in the clusters, which provides more reaction sites for future gelation. This promotes the formation of branched clusters of aerogel structures.

3.3.3 Effects of Catalyst Concentration

Previous investigations have shown that F^- has remarkable catalytic effects on the rate of condensation reactions (section 3.3.1). And further investigations about the effects of catalyst concentration in the third step during our proposed 3-step method sol-gel process on the aerogel's physical properties have been performed in our studies.

Five silica aerogels samples were prepared by varying molar ratio of NH_4F: Si from 0.002 to 0.01 while maintaining other parameters at constant values. Table 3.3.3 shows the properties of silica aerogels prepared from different molar ratios of NH_4F: Si during the third step. In the sample name, the number after F, N is the molar ratio of NH_4F: Si. It can be seen that, the aerogel's density, yield strength, and flexural modulus all decrease significantly with increasing molar ratios of NH_4F: Si. Among them, the molar ratios of NH_4F: Si at 0.006, 0.008 and 0.01 all yield silica aerogels with densities lower than 0.01 g/cm^3, out of which, only the molar ratio of NH_4F: Si at 0.01 retains volume higher than 90%. This shows that the formed gel structure is less affected by drying conditions and that the gel structure is sufficient strong to resist drying stress.
Recalling our previous results, we obtained thermal conductivities of 9~10 mW/m.K for all the five silica aerogels samples by hotwire measurements. This is again much lower than previously reported silica aerogels' thermal conductivity of 15 mW/m.K [3].

Similar analysis on the reduction ratios in yield strength and flexural modulus has been performed using the yield strength and flexural modulus of sample F,N,0.002-16E-0-0 as the reference values(P_0, E_0). Figure 3.3.7 shows the reduction ratios (P/P_0, E/E_0) vs. molar ratios of NH_4F: Si. From the plot, samples with molar ratios of NH_4F: Si at 0.006, 0.008 and 0.01 have improved ductile properties than the reference sample. Therefore, samples with higher the catalyst concentrations have improved ductile properties. Together with observations of solvent effects in Section 3.3.2, we propose that increase both molar ratios of EtOH: Si and NH_4F: Si could produce silica aerogels with improved ductility.

Table 3.3.3 Properties of silica aerogels prepared from different molar ratios of NH_4F: Si

Sample	Yield Strength (kPa)	Flexural Modulus (MPa)	Bulk Density (g/cm^3)	Porosity (%)	Volume Preserved Shrinkage (%)	Thermal Conductivity (mW/m.K)
F,N,0.002-16E-0-0	62.0+/-8.2	1.36+/-0.10	0.140+/-0.002	93.6	55.0	10.93 +/- 0.05
F,N,0.004-16E-0-0	33.7+/-7.1	0.85+/-0.03	0.121+/-0.002	94.4	68.5	10.02 +/- 0.02
F,N,0.006-16E-0-0	28.8+/-7.4	0.44+/-0.02	0.099+/-0.002	95.4	78.1	9.80 +/- 0.02
F,N,0.008-16E-0-0	24.4+/-5.2	0.42+/-0.01	0.095+/-0.002	95.6	87.1	9.81 +/- 0.04
F,N,0.01-16E-0-0	23.8+/-4.3	0.39+/-0.03	0.091+/-0.001	95.8	91.2	10.01 +/- 0.02

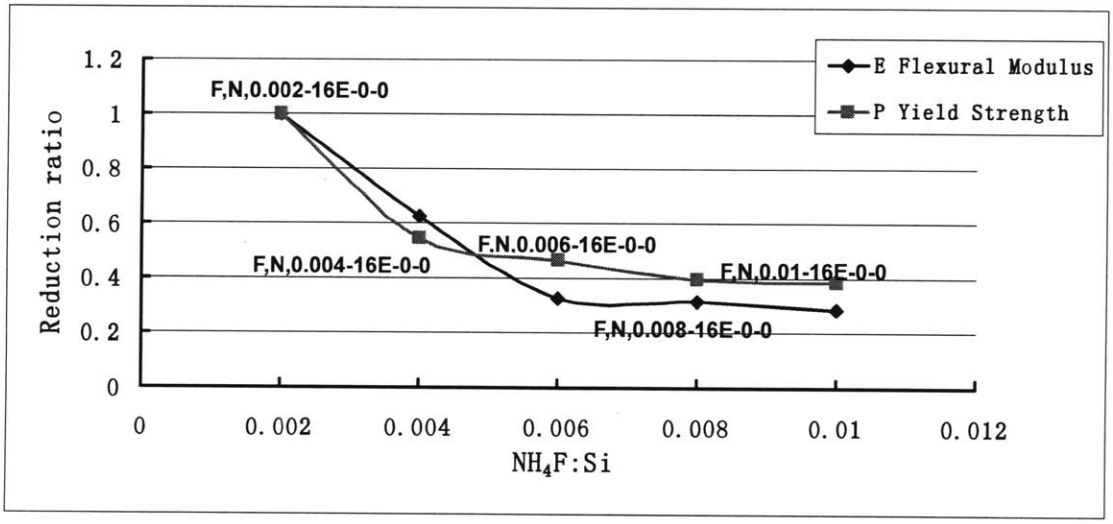

Figure 3.3.7 Reduction ratios in both yield strength and flexural modulus vs. molar ratio of NH_4F: Si

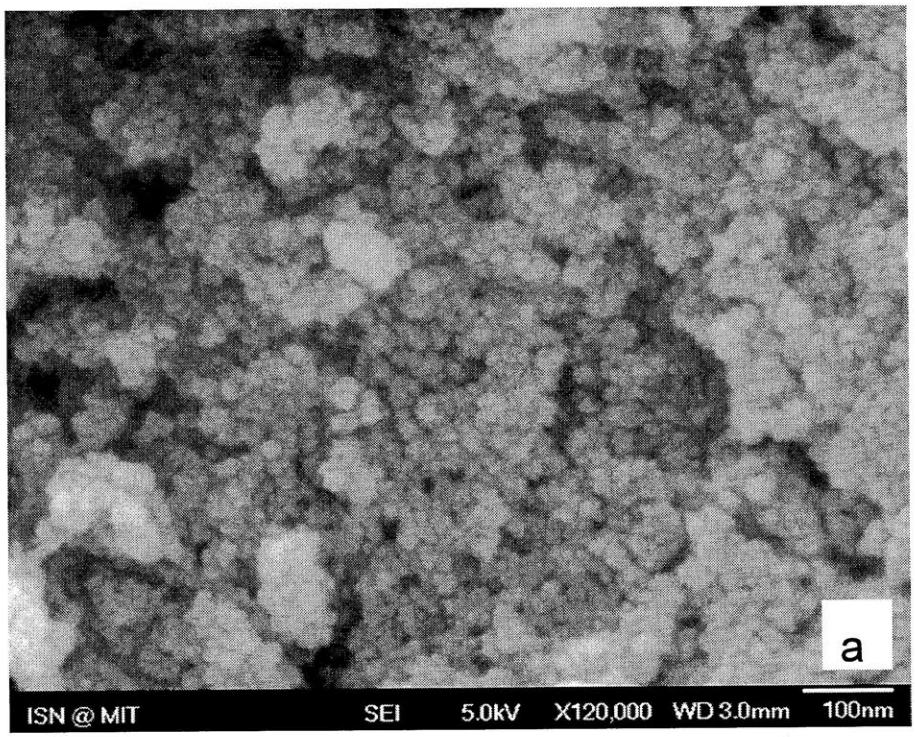
a
ISN @ MIT
SEI
5.0kV
X120,000
WD 3.0mm
100nm

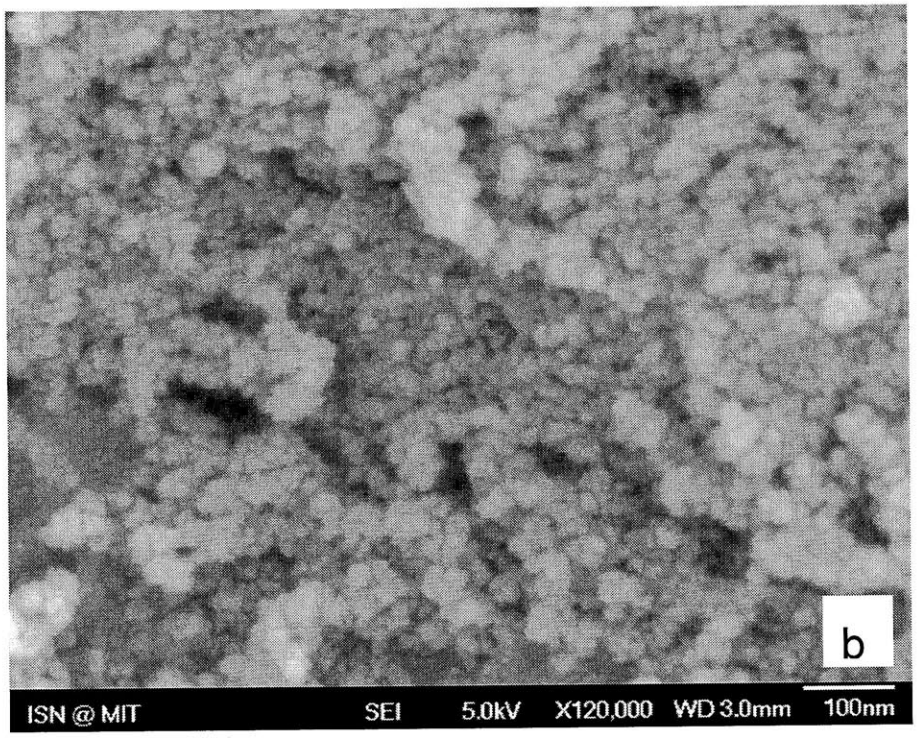
b
ISN @ MIT
SEI
5.0kV
X120,000
WD 3.0mm
100nm

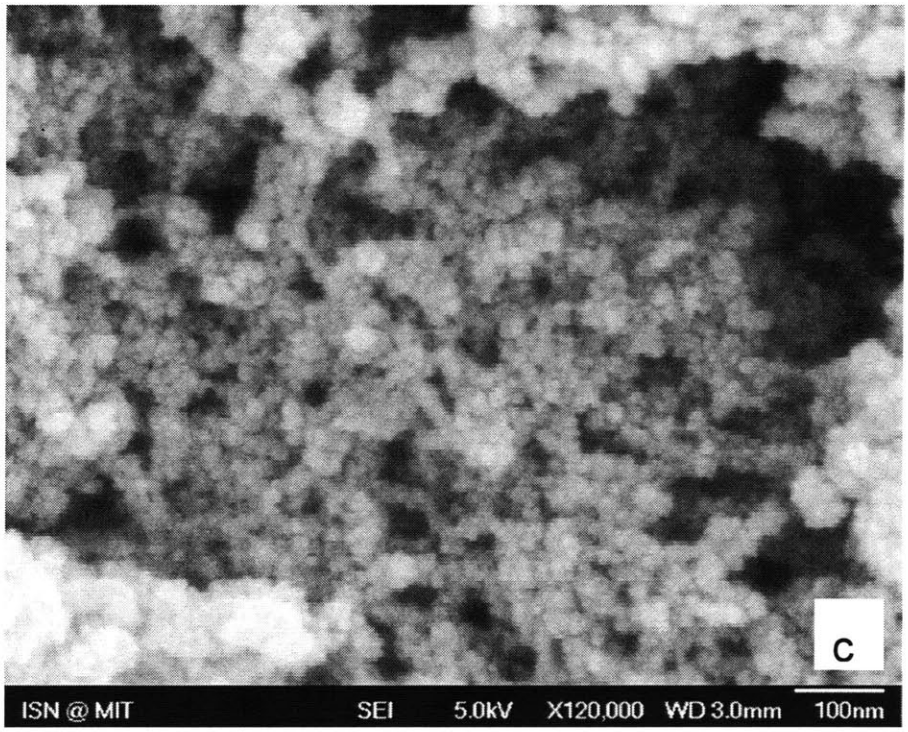
c
ISN @ MIT
SEI
5.0kV
X120,000
WD 3.0mm
100nm

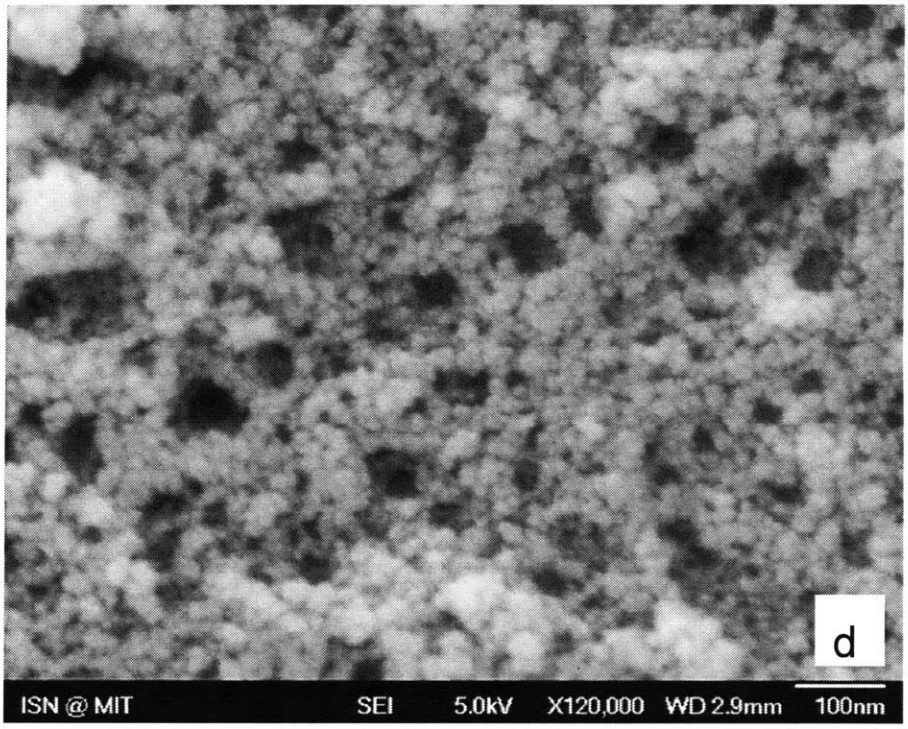
d
ISN @ MIT
SEI
5.0kV
X120,000
WD 2.9mm
100nm

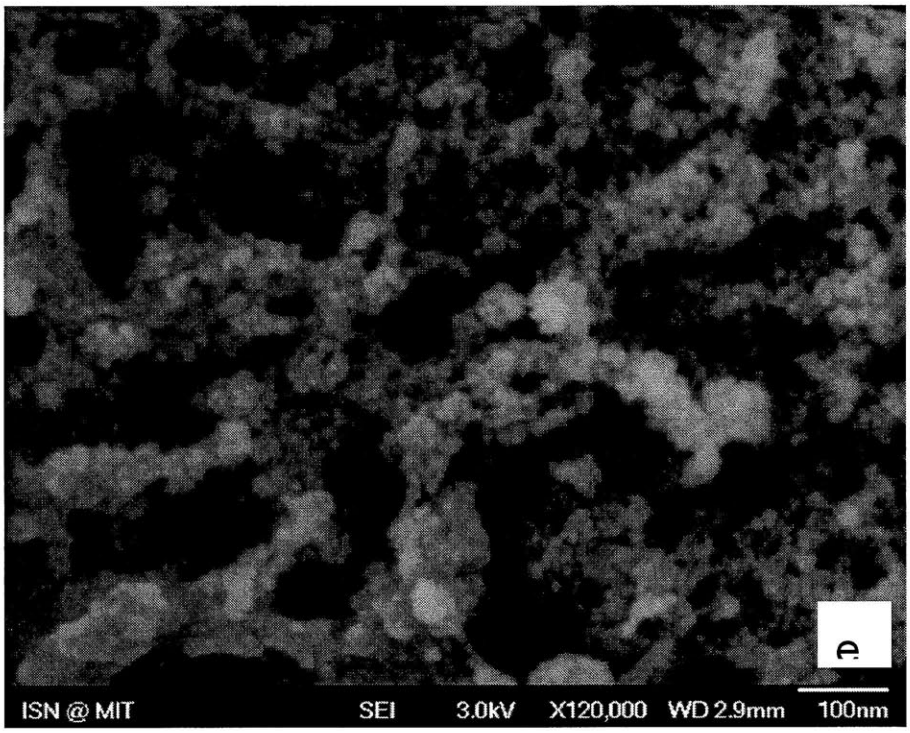

Figure 3.3.8 SEM images of silica aerogels samples prepared with various catalyst concentration: (a) F,N,0.002-16E-0-0, (b) F,N,0.004-16E-0-0, (c) F,N,0.006-16E-0-0, (d) F,N,0.008-16E-0-0, (e) F,N,0.01-16E-0-0.

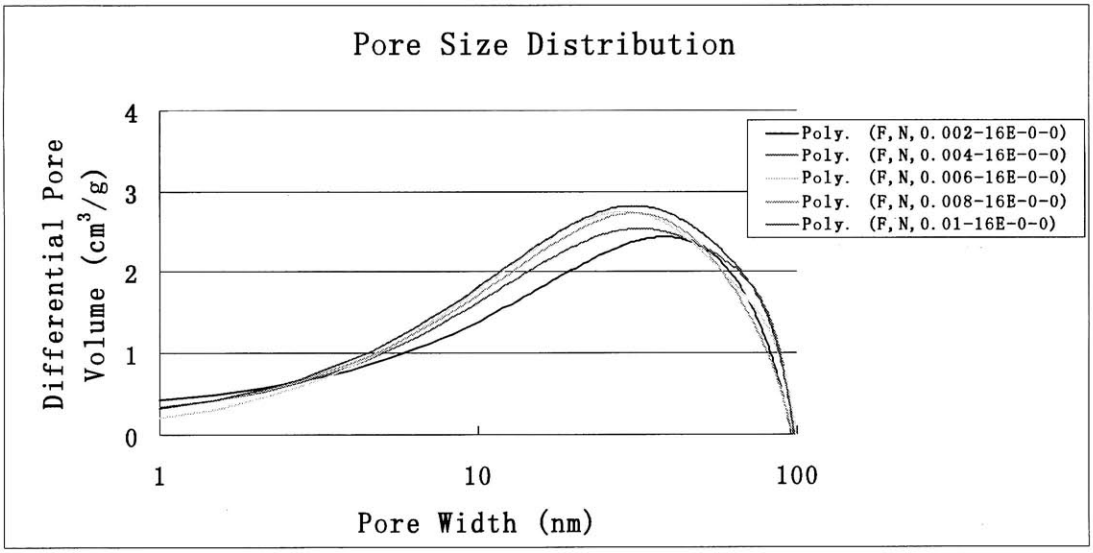

Figure 3.3.9 Pore size distribution of silica aerogels with various catalyst concentrations

Figure 3.3.8 presents the high magnification SEM images of silica aerogels prepared with various catalyst concentrations. As the catalyst concentration decreases, more compact gel structure, and increased connectivity among clusters, and fewer pores are observed, implying increased consolidation of secondary clusters. In Figure 3.3.9, the result of BET pore size distributions further confirms the changes in the porous feature as catalyst concentration decreases. It has been noticed that with decreasing catalyst concentration, pore volume decreases, thus, the density is increased, as shown in Table 3.3.3. Yet, broad pores size distributions (from several nanometers up to 100nm) still exist in all of the four samples.

Based on the above observations, we conclude that, higher catalyst concentration produces gel networks composed of highly branched polymeric clusters with looser connectivity and more pore volume. Loose connectivity among clusters results in reduction in both yield strength and flexural modulus, meaning an improved ductility.

Thermal conductivities of samples prepared from higher molar ratios of NH_4F: Si are relatively lower (see Table 3.3.3). We contribute the observed lower thermal conductivities of those samples to the gel networks which are mainly composed of less condensed clusters with loose connectivity. Highly branched polymeric clusters and loose connectivity reduce the solid conduction, leading to lower thermal conductivity. We also think that the slightly higher thermal conductivity of sample F,N,0.01-16E-0-0 is due to a higher gas conduction resulting from the air molecules inside larger pores (>70nm) (see Figure 3.3.8 (e)).

The effects on both of the yield strength and flexural modulus of silica aerogel by the molar ratio of NH_4F: Si can be explained by the catalytic effects of F^- on the condensation rate. F^- catalyzed condensations involves the displacement of OH^- with F^-, which is more electron-withdrawing than OH^-. The replacement of F^- with OH^- causes a reduction in the electron density of Si, thereby making nucleophilic attack from the other OH^- groups much easier to occur and increasing condensation rate. Also, a shorter

gelation time has been observed with increasing molar ratio of NH_4F: Si. Therefore, gel networks produced from higher molar ratios of NH_4F: Si are mainly composed of highly branched clusters with loose connectivity and larger pore volume, which contributes to lower yield strength and flexural modulus.

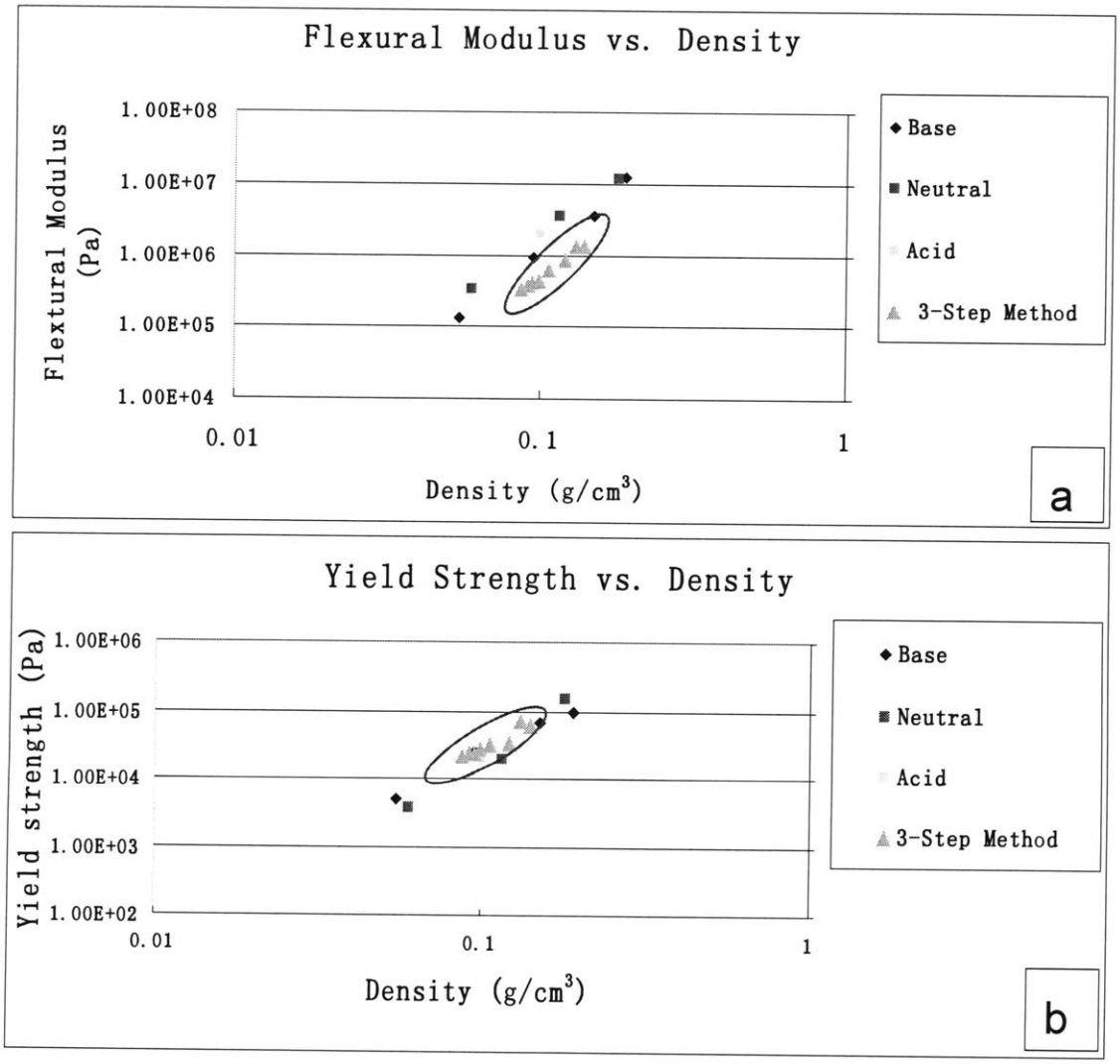

Figure 3.3.10 Comparison of mechanical properties with previously reported results [90]

3.3.4 Comparison of mechanical properties with others

To further demonstrate that silica aerogels produced by using the proposed 3-step method have much improved ductility, we compare both of the flexural modulus and yield strength from our samples with previously reported data [90]. Their silica aerogels were prepared under three different catalytic conditions: base, neutral or acid.

Figure 3.3.10 (a) shows the plot for flexural modulus comparison. We notice that the flexural modulus of our silica aerogels are all much lower (reduced by 50 ~80%) than the reported data within the same range of densities. Figure 3.3.10 (b) presents the yield strength of our silica aerogels. Our values are located in the similar region, yet, slightly higher than the reported data. Therefore, on the basis of the above comparison plots, we are confident that the ductility of silica aerogels produced by using the proposed 3-step method sol-gel process has been improved by 2~4 times.

3.3.5 Discussions on the extremely low thermal conductivities

Thermal conductivity measurements show that all of the silica aerogels prepared in our studies are much lower (see in Table 3.3.1 ~ 3.3.3) than previously reported value of 15 mW/m.K. We believe this is due to the hierarchical porous feature inside our silica aerogels' system. BET characterizations (see Figure 3.3.2, 3.3.6, and 3.3.9) show that the porous structure of our silica aerogels has a more broader pore size distributions than others(i.e. see Figure 3.3.11), and pores with diameters ranging from several nanometers to 100 nm all exist in our silica aerogels' system. Furthermore, more pore volume has been occupied by smaller pores (diameter<10nm) in our aerogels compared to others.

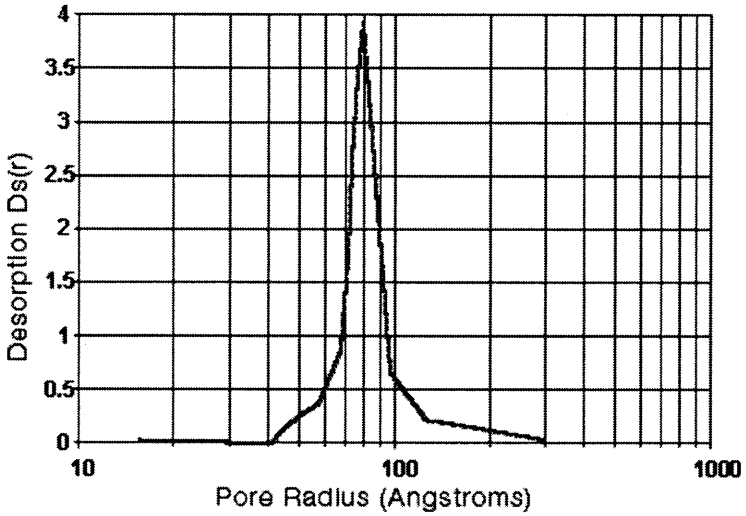

Figure 3.3.11 Pore size distribution of a single step silica aerogel with thermal conductivity of 17 mW/m.K[3]

As discussed in previous Section 2.2.2, the total thermal conductivity of silica aerogels consists of contributions from three parts: conduction through solid, conduction through gas and radiation though the particles/clusters and voids. The nanosized pores and particles/clusters are primarily responsible for the very low thermal conductivity of aerogels. However, lower thermal conductivity can be further reached by reducing the size of pores and minimizing the connectivity among particles/ clusters. Comparing the pore size distribution in Figure 3.3.10 with those of our silica aerogels in Figure 3.3.2, 3.3.6, and 3.3.9, we observe that more pore volume has been occupied by smaller pores with diameter of less than 10 nm in our silica aerogels' system benefiting from the broader range of pore size distribution. Those smaller pores could generate regions with much lower thermal conductivity within the entire hierarchical system, which limits the total gas heat conduction. Similarly, solid conduction could also be limited by the extremely small connections among particles/clusters. We thus believe those regions composed of smaller pores and loosely connected particles/clusters within the entire hierarchical porous structure of our silica aerogels limit the total heat transport and contribute to the extremely low thermal conductivities.

3.4 Conclusions

We propose a new 3-step method for sol-gel process, which provides better control of the clusters growth and formation of gel network. For the 3-step method, we employ three different catalysts to realize individual controls for hydrolysis, condensation and gelation. Silica aerogels with good quality in terms of low density, low thermal conductivity, improved ductility and better mechanical integrity have been produced. On the whole, the ductility of the silica aerogels produced by using the proposed 3-step method has been improved by 2~4 times.

Further investigations on the effects of sol-gel processing parameters on physical properties of silica aerogels have also been conducted by preparing samples with various solvent concentrations and catalyst concentrations through the proposed 3-step method. Experimental results have been consistently explained on the basis of SEM and BET characterizations.

Finally, we conclude that: (1) gel structure composed of larger pore volume, highly branched polymeric secondary clusters with loose connectivity contributes to silica aerogels' ductility; (2) larger pores (>70nm), consolidation of secondary clusters, and increased connectivity among clusters produce higher thermal conductivity; (3) the smaller pores and loosely connected particles/clusters within the entire hierarchical porous structure of our silica aerogels limit the total heat transport and contribute to the extremely low thermal conductivities.

4. Enhancement of the mechanical properties of silica aerogels through structure modification

4.1 Introduction

Silica aerogels are open-cell porous materials with extraordinary low thermal conductivity (0.015W/mK)[3], even lower than still air (0.025w/mK), making them desired for structural thermal insulations. However, the fragility of silica aerogels makes them impractical for structural applications although it has been created for over 70 years. Therefore, making silica aerogels mechanically robust is critical for promoting their applications.

Mostly, silica aerogels are produced from sol-gel process, which provides extensive opportunities for structure modifications of the gel network, thus, making silica aerogels more robust for applications. Silica aerogels have extremely high surface area(~1000m^2/g) and high porosity (>90%), so the structure modification can be considered as surface modification as well. Until now, two different kinds of methods have been developed for surface modifications of silica aerogels: (1) Surface derivatization method and (2) Co-precursor method [48]. For the surface derivatization method, wet silica gels are formed first, and then kept into aging solutions containing a mixture of solvent and the surface-modifying agent. Later on, mass transfer takes place through infiltration process leading to cross-linkings between silica skeleton and surface-modifying agent. Professor Leventis leads this research by incorporating organic cross-linkers, such as epoxides[55, 56] and polystyrene[57-59], into the gel network. The covalent bondings formed between the silica skeleton and the organic crosslinkers couldl dramatically increase the strength of the resulting aerogels. But, those polymer-cross-linked aerogels usually have higher densities (i.e. 0.44g/cm^3) and lower BET surface area (i.e. 171 m^2/g)[91], thus reduction in thermal insulation ability is expected. Besides, huge amounts of solvent and long process time are required to

achieve complete solvent exchange and subsequent surface modifications, and it is very costly. For the co-precursor method, surface modifying agents or certain functional materials are added into the sol as co-precursors before gelation. Thus, comparing to the surface derivatization method, co-precursors method could produce gels with uniformly modified the surface structures contributing to high integrity in bulk properties, yet, requires less process time. Aspen Aerogels has been focusing on fabrication of fiber reinforced silica aerogels. So far, their production of mechanically robust, flexible aerogel blankets with lower thermal conductivity(~0.014W/mK) are made of both inorganic and organic aerogels supported by meshes of polyimides (i.e., Nylon®), glass fibers, and many other materials[62-64]. However, instead of monolithic aerogels, silica granules are filled inside the aerogels' blanket and the continuously released aerogels' dust is hazardous.

In Section 3, we proposed a 3-step method for sol-gel processing, which has been experimentally examined to be able to produce silica aerogels with improved ductility. Here, we further investigate and demonstrate the ability of enhancing mechanical properties of silica aerogels through structure modification by using 3-step method. During the preparation of the modified silica aerogels, a small amount of water-soluble inorganic synthetic nanocomposite (Laponite® RDS) is added. The molecular-level synergism between silica nanoparticles and the functional nanocomposite inverts the relative host-guest roles in resulting aerogels' composite, leading to new stronger and more robust low-density materials. After being dried with supercritical CO_2, the modified silica aerogels have been characterized by 3-point bending, transient hotwire measurements, scanning electron microscopy (SEM), and Brunauer, Emmett and Teller (BET) method. Improved ductility and lower thermal conductivities have been observed. The effects of doped Laponite® RDS content on the microstructure and physical properties of prepared modified silica aerogels have been investigated and discussed.

4.2 Experimental

4.2.1 Preparation Methods of silica aerogels

4.2.1.1 Materials

Tetraethyl orthosilicate (TEOS, ≥98.0% (GC)) and ammonia standard solution(2.0 M in ethanol) were purchased from Sigma-Aldrich and used as received. Deionized water was obtained from Ricca Chemical Company. Anhydrous ethanol (ACS/USP grade) was from Pharmoco-Aaper Inc. Other materials were: hydrochloric acid (0.05 M) from ARISTAR and ammonium fluoride (1 M) from Acros Organics, both in the form of deionized water solutions. Laponite® RDS was obtained from Southern Clay Products, Inc. For supercritical drying, liquid carbon dioxide tank with siphon tube was purchased and used as received from Airgas. Inc

4.2.1.2 Procedure

In this study, silica aerogels' sample (F,N,0.01-16E-0-0) without modification was prepared using previously described 3-step method (Section 3.2). For the first step, the precursor solution was placed for hydrolysis with substoichiometric water under acid condition for 1.5h and the molar ratios of starting materials TEOS : EtOH : H_2O : H^+ were kept at 1 : 3 : 1 : 7 10^{-4}. During the second step, additional EtOH, water and ammonia solution were added to increase molar ratios of TEOS: EtOH: H_2O: $NH_3 \cdot H_2O$ to be 1:16: 4: 2 10^{-3}, stirring for 0.5h. For the third step, 1ml ammonium fluoride (1M) was added as gelation agent and sol solutions were poured into molds before gelation point.

For the preparations of the modified silica aerogels' samples, the binder (Laponite® RDS) was first dissolved into water to form dispersed solution (10wt % and 20wt %). 3-step method was also employed in this experiment set. The first step was the same as described previously. In the second step, after the additions of EtOH, water and ammonia solution, binder's solution(1ml, 3ml, or 5ml of 10wt % for sample F, N,

0.01-16E-0.1-20, F, N, 0.01-16E-0.3-20, or F, N, 0.01-16E-0.5-20, respectively, and 5ml 20wt% for sample F, N, 0.01-16E-1.0 -20) was added by keeping the molar ratios of TEOS: EtOH: H_2O: $NH_3 \bullet H_2O$ constant at 1:16: 4: 2 10^{-3}. The mixture sol solution was then ultrasonically dispersed for 20 min, following with stirring for another 10 min. During the third step, 1ml ammonium fluoride (1M) was added as gelation agent and sol solutions were poured into molds prior to gel point. All the wet gels obtained were first aged for three days under ethanol and then washed three times with fresh ethanol, with 24h interval. After being dried by supercritical CO_2, all the samples were ready for further investigations.

4.2.2 Methods of Characterizations

Same as described in Section 3.2.2.

4.3 Results and Discussions

Samples with various binder's concentration were prepared by keeping all the other sol-gel synthesis parameters at constant values. Table 4.3.1 gives the properties of the prepared binder modified silica aerogels. It can be seen that, as the binder's concentration increases, aerogel's density, yield strength, and flexural modulus increase. Slight decreases in sample F,N,0.01-16E-0.5-20 may come from the non-uniform dispersion of the binder clusters in the sol solution prior to gelation, due to increasing number of binder condensates at higher binder's concentration. Hotwire measurements show that thermal conductivities of all the prepared silica aerogels vary from 10 to 11 mW/m.K, much lower than previously reported silica aerogels' thermal conductivity of 15 mW/m.K [3]

Table 4.3.1 Properties of silica aerogels prepared from different binder's concentration

Sample	Weight Percentage of Binders (wt%)	Yield Strength (kPa)	Flexural Modulus (MPa)	Bulk Density (g/cm^3)	Thermal Conductivity (mW/m.K)
F,N,0.01-16E-0-0	0	23.8+/-4.3	0.39+/-0.03	0.091+/-0.001	10.01+/-0.02
F,N,0.01-16E-0.1-20	1.34	35.3+/-3.5	0.58+/-0.03	0.108+/-0.002	10.28+/-0.03
F,N,0.01-16E-0.3-20	4.46	58.9+/-2.4	1.34+/-0.05	0.122+/-0.002	10.59+/-0.02
F,N,0.01-16E-0.5-20	5.9	54.3+/-3.6	1.22+/-0.11	0.123+/-0.002	10.72+/-0.03
F,N,0.01-16E-1.0-20	13.7	62.9+/-2.5	2.50+/-0.11	0.155+/-0.006	11.07+/-0.04

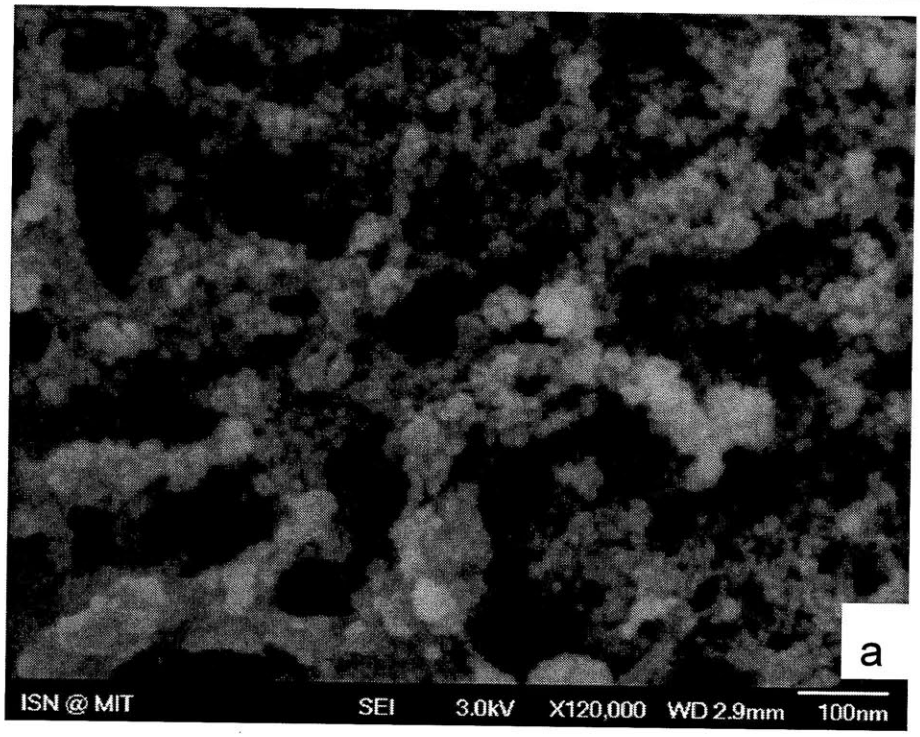

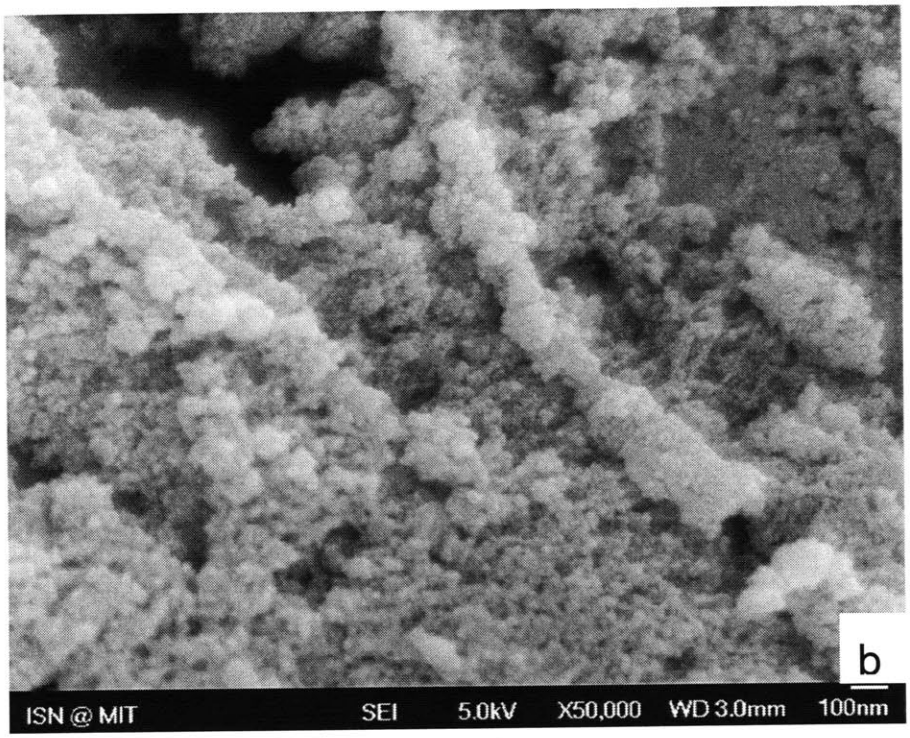
b
ISN @ MIT
SEI
5.0kV
X50,000
WD 3.0mm
100nm

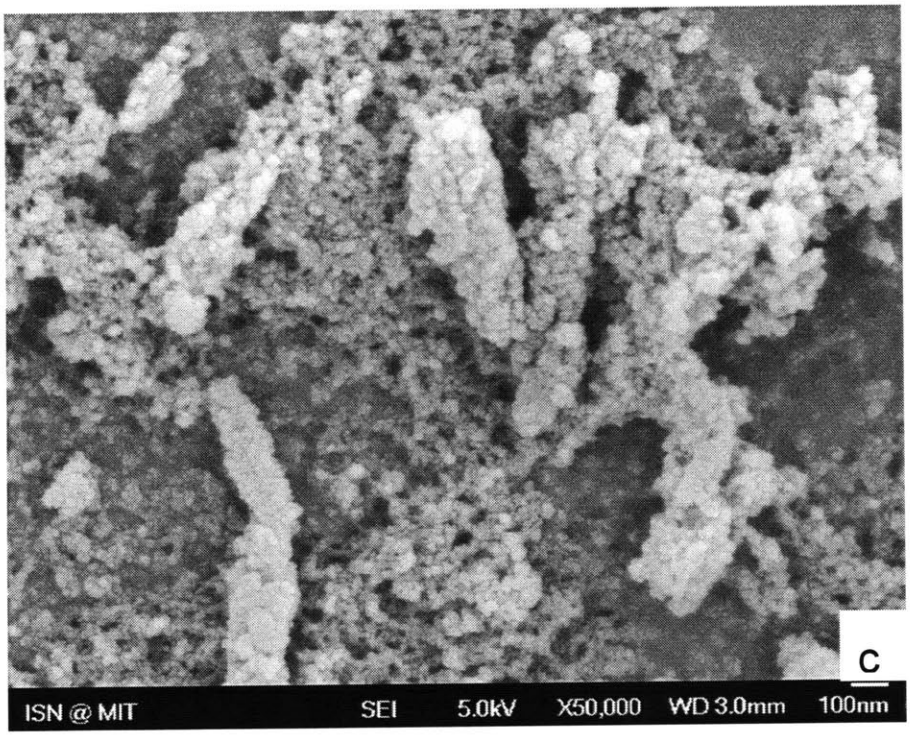
c
ISN @ MIT
SEI
5.0kV
X50,000
WD 3.0mm
100nm

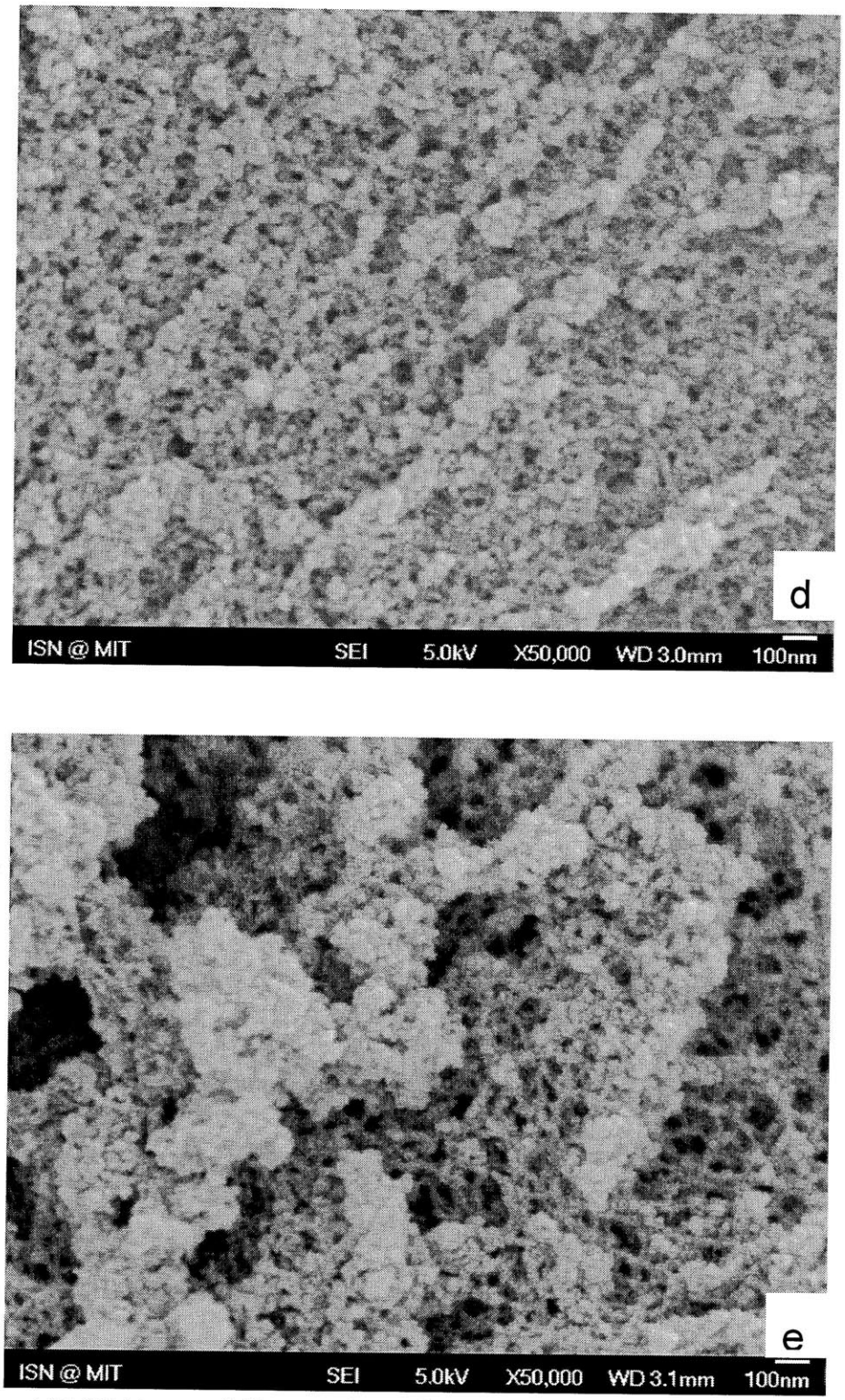

Figure 4.3.1 SEM images of silica aerogels samples prepared with various binders concentration: (a) F,N,0.01-16E-0-0, (b) F,N,0.01-16E-0.1-20, (c) F,N,0.01-16E-0.3-20, (d) F,N,0.01-16E-0.5-20, (e) F,N,0.01-16E-1.0-20.

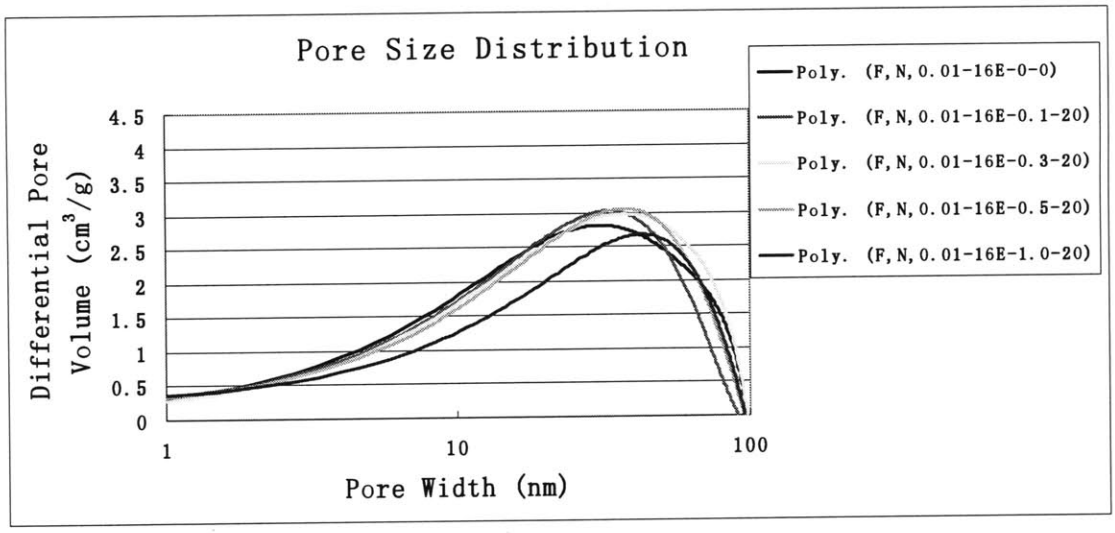

Figure 4.3.2 Pore size distribution of silica aerogels with various binder's concentration.

Figure 4.3.1 shows the SEM images of the silica aerogels prepared by varying binder's concentrations, and the differences in the porous feature among these samples are presented. In Figure 4.3.1 (a), gel networks consisting of larger pores, highly branched polymeric clusters with loose connectivity are formed by using the 3-step method. On the basis of previous discussions in Section 3.3, these structure features contribute to lower yield strength and flexural modulus of silica aerogels. From Figure 4.3.1 (b)~(d), gel networks with doped binders (Laponite® RDS) content are observed and binders exist in the form of larger and extremely condensed cylindrical clusters surrounded by cross-linked porous gel structure. As the binder's concentration increases, increasing in the number of the binder clusters is observed. It is worth to point out that, despite the existence of the doped binders, highly cross-linked porous structures composed of less condensed silica clusters with loosely connected network are preserved in all the binder modified aerogel samples. In Figure 4.3.2, BET pore size distributions further confirm the observations on the porous feature from SEM. Broad pores size distributions (from several nanometers up to 100nm) are observed in all the five samples, corresponding to the highly cross-linked porous structures. However, it has been noticed that as the binder' concentration increases, pore volume decreases,

thus, resulting in increased densities.

To investigate the enhancements of the ductile properties of the binder modified silica aerogels, we compare both of the flexural modulus and yield strength with previously reported data [90](see Figure 4.3.3). The reported silica aerogels were prepared under three different catalytic conditions, base, neutral or acid, and the mechanical properties were tested by using 3-point bending, which has also been employed in our testings. Figure 4.3.3 (a) shows the plot for flexural modulus comparison. We notice that the flexural modulus values of our silica aerogels are all much lower than the reported values with the same range of densities. Nevertheless, the plot for yield strength comparison in Figure 4.3.3 (b) shows that the yield strength values of our silica aerogels are located around the same region, yet, slightly higher than the reported values. Therefore, based on the two plots, we are confident that the ductility of silica aerogels produced in our studies has been improved. However, sample F, N, 0.01-16E-1.0 -20 with the largest binder's concentration doesn't give too much improvement in the ductility comparing to others.

From the transient hotwire measurements (see Table 4.3.1), extremely low thermal conductivities have been reached in all the five samples. Slight increases in the thermal conductivities of the samples with higher binder's concentrations have been noticed, which could be contributed to the increasing numbers of binder's condensates. With the presence of highly consolidated cylindrical binder's condensates, solid conduction is enhanced, contributing to the total heat transport, thus, resulting in higher thermal conductivities. Yet, highly porous gel structures composed of less condensed silica clusters with loosely connected networks are preserved in all the binder modified samples. We believe it is the gel networks consisting of the unique porous feature that limit the total heat transport, contributing to the extremely low thermal conductivities (see more detailed discussions in Section 3.3.5).

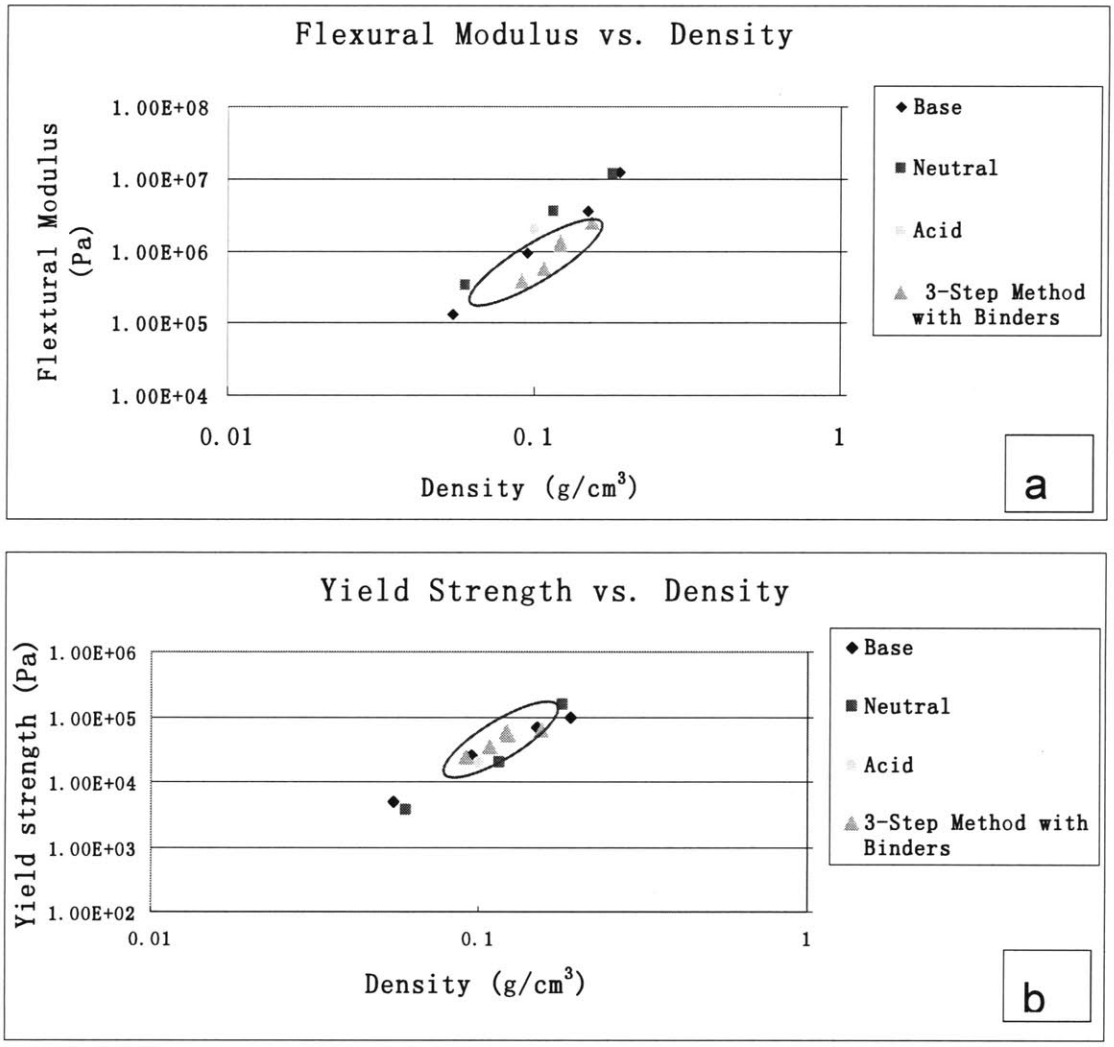

Figure 4.3.3 Comparison of mechanical properties with previously reported results [90]

The enhancements of the ductile properties of silica aerogels could be explained by the effects of doped Laponite® RDS content on the microstructure of the prepared binder modified silica aerogels.

Laponite® RDS is a sol forming grade of synthetic layered crystalline silicate incorporating an inorganic polyphosphate (TSPP) as dispersion agent. When dissolved in water, colourless, translucent and colloidal, low viscosity dispersions known as sols are formed. Laponite has a layer structure which, in dispersion in water, is in the form of

two-dimensional disc-shaped crystals, with the empirical formula of single crystal unit as shown in Figure 4.3.4. This shows six octahedral magnesium ions sandwiched between two layers of four tetrahedral silicon atoms. These groups are balanced by twenty oxygen atoms and four hydroxyl groups. When Laponite® RDS powder is added into water, the blended TSPP dissolves, the pyrophosphate $(P_2O_7)^{4-}$ anions become associated with the positively charged edges of the Laponite crystal, making the whole particle negatively charged. This is subsequently surrounded completely by a loosely held layer of hydrated sodium ions, whose positive charges cause mutual repulsions between the dispersed Laponite crystals. Thus, stable Laponite sol dispersion is formed. When a sol dispersion of Laponite is added into solution containing simple salts, surfactants, other solvents, or soluble impurities, the dispersing effect of the TSPP is rapidly overcome as the pyrophosphate anions are absorbed by the other compounds. At this time, adjacent Laponite crystals will begin to interact with each other and the "house of cards" type structure can form(see Figure 4.3.5), resulting in viscosity increase of the entire solution[92]. This unique feature of Laponite gives the opportunity to modify materials at the microstructure level.

During our preparation of binder modified silica aerogels, the Laponite sol dispersion was added during the second step of sol-gel process. By the end of first step for hydrolysis, small reactive silanol oligomers were presented in the sol solution. Upon the addition of Laponite dispersion, the dispersing effect of the TSPP was overcome as the pyrophosphate anions were absorbed by the solvent and newly formed silanol oligomers. Then, the adjacent Laponite® crystals began to interact with each other and condensates with the "house of cards" structure were formed, corresponding to the larger and extremely condensed cylindrical clusters seen in SEM images. Ultrasonication was employed to promote formation of uniform sol mixture.

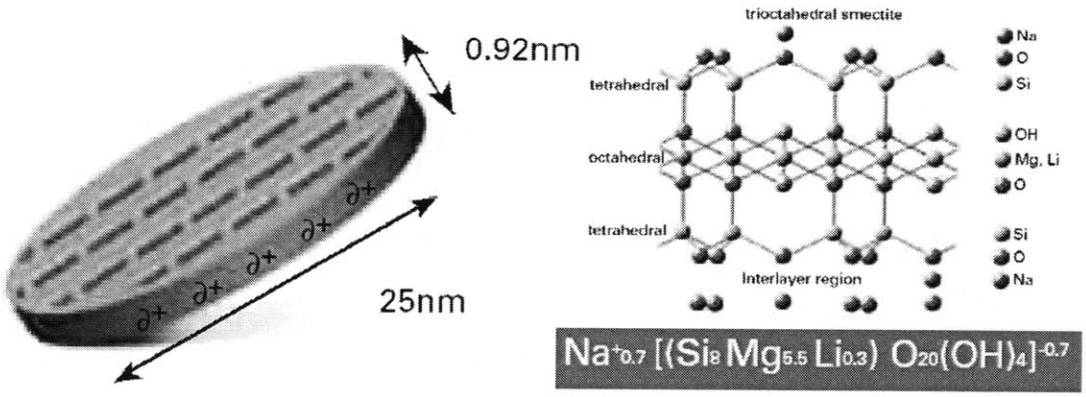

Figure 4.3.4 Single crystal (left) and molecular structure (right) of Laponite[92]

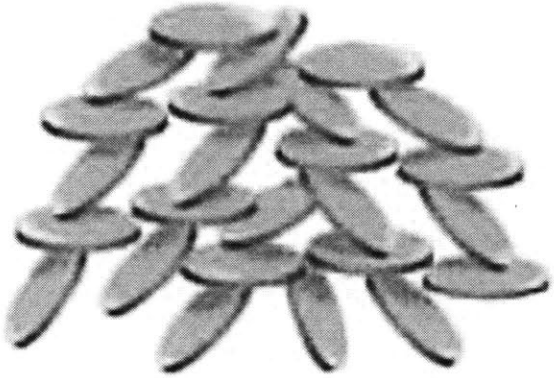

Figure 4.3.5 Formation of "House of Cards" [92]

Significant increase in viscosity of the sol solution was observed. In the third step, with the addition of NH_4F to induce gelation, wet gels were formed and then dried under supercritical CO_2.

We believe the Laponite® crystals interact with the silica network in two ways: (1) the crystals stack together and are formed in a "house of cards" structure through electrostatic bonds, resulting in the formation of larger highly condensed clusters(Laponite condensates) observed in SEM; (2) the hydroxyl groups on the surface of the Laponite condensates bond with hydrolyzed silanols, so that the condensates are surrounded by cross-linked porous structure. Bondings between the Laponite

condensates unlikely occur due to the limited number of hydroxyl groups on the surface.

The Laponite condensates, consisting of high consolidation structure, contribute to the enhancements in both yield strength and flexural modulus the binder modified silica aerogels In the binder modified structures, the surrounded porous silica networks link all the laponite condensates together to form bulk composite. The surrounded porous structure provides more space for the movements of silica clusters and Laponite condensates with response to external loading, contributing to the flexibility. Thus, overall, at lower binder concentrations, we observe improved ductility in the binder modified silica aerogels. However, due to the lack of bonding between the doped Laponite condensates, the yield strength will increase less than the flexural modulus. Therefore, at higher binder concentrations, the binder modified aerogels, such as F, N, 0.01-16E-1.0-20, doesn't show too much improvement in the ductile properties comparing to others at lower binder concentrations.

4.4 Conclusions

We have demonstrated the ability of enhancing mechanical properties of silica aerogels through structure modification by using 3-step method. Laponite® RDS, a water soluble silicate was incorporated into the sol-gel synthesis of silica aerogels as structure modifying agent. And, silica aerogels with improved ductile properties have been produced. Furthermore, extremely low thermal conductivities have been retained in all the prepared samples benefiting from the preservation of highly cross-linker porous structures. Explanations of the observations have been discussed and supported on the basis of SEM and BET characterizations.

5. Future Research

Further structure modifications of silica aerogels through addition of binders (organic cross-linkers, such as, cellulosic macromolecules) using 3-steps sol-gel processing are going to be investigated and in depth understandings on the modification mechanism of gel structures are anticipated.

Composite panels with silica aerogels as fillings and low volume fraction of core (honeycomb or truss assembly) as supports are also going to be studied and fabricated , following with thermal conductivity measurements under ambient pressure as well as at reduced pressure (1/3atm).

Investigations on the radiation component of silica aerogel's heat transfer are going to be performed by measuring transmissivity of silica aerogel in near to far infrared region.

References

[1] S.S. Kistler, Coherent expanded aerogels and jellies, Nature 127 (1931), pp.741;

[2] J. Kahn, Lightweight aerogels can make a solid contribution to energy conservation, LBL Research Reviews (1991), Summer, pp.3;

[3] http://eetd.lbl.gov/ECS/aerogels/sa-physical.html from Microstructured Materials Group at Lawrence Berkeley National Laboratory.

[4] M. Cantin, M. Casse, L. Koch, R. Jouan, P. Mestreau, D. Roussell, F. Bonnin, J. Moutel, S.J. Teichner, Silica aerogels used as Cherenkov radiators, Nuclear Instruments and Methods 118 (1974), pp.177;

[5] V. Gibiat, O. Lefeuvre, T. Woignier, J. Pelous, and J. Phalippou, Acoustic properties and potential applications of silica aerogels, Journal of Non-Crystalline Solids 186 (1995), pp.244;

[6] M. Gonauer, J. Fricke, Acoustic properties of microporous SiO_2-aerogel, Acustica 59 (1986), pp.177;

[7] V. Wittwer, Development of aerogel windows, Journal of Non-Crystalline Solids145 (1992), pp.233;

[8] H.D. Gesser, P.C. Goswami, Aerogels and related porous materials, Chemical Reviews 89 (1989), pp.765;

[9] J. Fricke, T. Tillotson, Aerogels: Production, characterization, and applications, Thin Solid Films 297 (1997), pp.212;

[10] N. Husing, U. Schuber, Aerogels-Airy Materials: Chemistry, Structure, and Properties, Angewandte Chemie International Edition 37 (1998), pp.22;

[11] A.C. Pierre, G.M. Pajonk, Chemistry of aerogels and their applications, Chemical Reviews, 102 (2002), pp.4243;

[12] Y.K. Akimov, Fields of application of aerogels (Review), Instruments and Experimental Techniques, 46 (2003), pp.287;

[13] P.M. Norris, S. Shrinivasan, Aerogels: Unique material, fascinating properties and unlimited applications, Annual Review of Heat Transfer, 14 (2005), pp.385;

[14] C.J. Brinker and G.W. Scherer, Sol-Gel Science: The Physics and Chemistry of Sol-Gel Processing (Academic Press, Inc.: New York, 1990);

[15] J.D. Wright and N. A.J.M. Sommerdijk, Sol-Gel Materials Chemistry and

Applications (Gordon and Breach Science Publishers, 2001),

[16] C.J. Brinker, K.D. Keefer, D.W. Schaefer, C.S. Ashley, Sol-gel transition in simple silicates, Journal of Non-Crystalline Solids 48 (1982), pp.47;

[17] T. Woignier, J. Phalippou, R. Vacher, Parameters affecting elastic properties of silica aerogels, Journal of Materials Research 4 (1989), pp.688;

[18] J. Fricke, Aerogels, Scientific American 256(5) (1988), pp. 92;

[19] P. Scheuerpflug, R. Caps, D. Buttner, and J. Fricke, Apparent thermal conductivity of evacuated SiO_2-Aerogel tiles under variation of radiative boundary-conditions, International Journal of Heat and Mass Transfer 28 (1985), pp. 2299.

[20] J. Zarzycki, M. Prassas, and J. Phalippou, Synthesis of glasses from gels - the problem of monolithic gels, Journal of Materials Science 17(1982), pp.3371.

[21] S.H. Wang and L.L. Hench, in Better Ceramics Through Chemistry, MRS Symposia Proceedings 32, eds, C.J. Brinker, D.E. Clark, and D.R. Ulrich(North-Holland, New York, 1984), pp.71;

[22] G. Orcel, and L.L. Hench, in Better Ceramics Through Chemistry, MRS Symposia Proceedings 32, (1984), eds, C.J. Brinker, D.E. Clark, and D.R. Ulrich(North-Holland, New York, 1984), pp.79;

[23]http://en.wikipedia.org/wiki/File:Carbon_dioxide_pressure-temperature_phase_diagram.svg

[24] S. K. Kang, and S. Y. Choi, Synthesis of low-density silica gel at ambient pressure: Effect of heat treatment, Journal of Materials Science 35 (2000), pp. 4971;

[25] A.P. Rao, G..M. Pajonk, A.V. Rao, Effect of preparation conditions on the physical and hydrophobic properties of two step processed ambient pressure dried silica aerogels, Journal of Materials Science 40 (2005), pp. 3481;

[26] T.Y. Wei, T. F. Chang, and S.Y. Lu, Preparation of monolithic silica aerogel of low thermal conductivity by ambient pressure drying, Journal of the American Ceramic Society, 90(2007), pp. 2003;

[27] R.K. Iler, The Chemistry of Silica (Wiley, New York, 1979), pp. 21;

[28] W. Mahler and M. Bechtold, Freeze-formed silica fibers, Nature, 285(1980), pp.27;

[29] T. Maki and S. Sakka, Formation of alumina fibers by unidirectional freezing of gel, Journal of Non-Crystalline Solids 82 (1986), pp.239;

[30] B.B. Mandelbrot, Fractals, Form and Chance (Freeman, San Francisco, 1977);

[31] S. Sakka, in Better Ceramics Through Chemistry, eds, C.J. Brinker, D.E. Clark, and D.R. Ulrich (North-Holland, New York, 1984), pp. 91;

[32] S. Sakka, K. Kamiya, K. Makita, and Y. Yamamoto, Formation of sheets and coating films from alkoxide solutions, Journal of Non-Crystalline Solids 63 (1984), pp.223;

[33] S. Sakka and K. Kamiya, The sol-gel transition in the hydrolysis of metal alkoxides in relation to the formation of glass-fibers and films, Journal of Non-Crystalline Solids 48 (1982), pp.31;

[34] H. Tsuchida, Science of Polymers (Baihukan, Tokyo, 1975), pp.85;

[35] W. Stober, A. Fink, and E. Bohn, Controlled growth of monodisperse silica spheres in micron size range, Journal of Colloid and Interface Science 26 (1968), pp.62;

[36] K.A. Mauritz,; R.F. Storey,; C.K. Jones, Multiphase Polymer Materials: Blends, Ionomers, and Interpenetrating Networks, eds. L.A. Utracki and R.A. Weiss, ACS Symp. Ser. No. 395; (American Chemical Society: Washington, DC, 1989) pp.401;

[37] M.G. Voronkov, V.P Mileshkevich, and Y.A Yuzhelevki, The Siloxane Bond (Consultants Bureau, New York, 1978);

[38] E.R. Pohl and F.D. Osterholtz in Molecular Characterization of Composite Interfaces, eds. H. Ishida and G.. Kumar (Plenum, New York, 1985), pp.157;

[39] K.J. McNeill, J.A. DiCaprio, D.A. Walsh, and R.F. Pratt, Kinetics and mechanism of hydrolysis of a silicate triester, tris(2-methoxythoxy)phenylsilane, Journal of the American Chemical Society 102(1980), pp.1859;

[40] R. Aelion, A. Loebel, and F. Eirich, Hydrolysis of ethyl silicate, Journal of the American Chemical Society 72 (1950), pp.5705;

[41] R. Aelion, A. Loebel, and F. Eirich, The hydrolysis and polycondensation of tetra-alkoxysilanes, Recueil Travaux Chimiques Des Pays-Bas – Journal of the Royal Netherlands Chemical Society 69 (1950), pp.61;

[42] http://www.psrc.usm.edu/mauritz/solgel.html;

[43] K.D. Keefer, in: Silicon Based Polymer Science: A Comprehensive Resource; eds. J.M. Zeigler and F.W.G. Fearon, ACS Advances in Chemistry Ser. No. 224, (American Chemical Society: Washington, DC, 1990) pp.227.

[44] R.J.P. Corriu, D. LeClercq, A. Vioux, M. Pauthe, and J. Phalippou in Ultrastructure Processing of Advanced Ceramics, eds. J.D. Mackenzie and D.R. Ulrich (Wiley, New York, 1988), pp. 113;

[45] E.M. Rabinovich and D.L. Wood in Better Ceramics Through Chemistry II, eds. C.J. Brinker, D.E. Clark, and D.R. Ulrich (Materials Research Society, Pittsburgh, 1986), pp.251;

[46] R.T. Morrison and R.N. Boyd, Organic Chemistry (Allyn & Bacon, Boston, 1966);

[47] R.K. Iler, The Chemistry of Silica (Wiley, New York, 1979);

[48] A. S. Dorcheh, M.H. Abbasi, Silica aerogel; synthesis, properties and characterization, Journal of Materials Processing Technology 199 (2008), pp.10;

[49] S.D. Bhagat, Y.-H. Kim, Y.-S. Ahn, and J.-G. Yeo, Textural properties of ambient pressure dried water-glass based silica aerogel beads: One day synthesis, Microporous and Mesoporous Materials. 96 (2006), pp.237;

[50] S.D. Bhagat, Y.-H. Kim, Y.-S. Ahn, and J.-G. Yeo, Rapid synthesis of water-glass based aerogels by in situ surface modification of the hydrogels, Applied Surface Science 253 (2007), pp.3231;

[51] N. Leventis, I. A Elder, D. R. Rolison, M. L.Anderson, and C.Merzbacher, Durable modification of silica aerogel monoliths with fluorescent 2,7-diazapyrenium moieties. Sensing oxygen near the speed of open-air diffusion, Chemistry of Materials 11(1999), pp.2837.

[52] N. Leventis, I. A. Elder,; G. J. Long, D. R. Rolison, Using nanoscopic hosts, magnetic guests, and field alignment to create anisotropic composite gels and aerogels, Nano Letters 2(2002), pp.63;

[53] N. Leventis, C. Sotiriou-Leventis, G.H. Zhang, and A. M. Rawashdeh, Nanoengineering strong silica aerogels, Nano Letters 2(2002), pp.957;

[54] http://www.aerogel.org/

[55] N. Gupta and W. Ricci, Processing and compressive properties of aerogel/epoxy composites Journal of Materials Processing Technology 198(2008), pp.178;

[56] M. A. B. Meador, E. F. Fabrizzio, F. Ilhan, A. Dass, G. Zhang,; P. Vassilaras, J. C. Johnston, N. Leventis, Cross-linking amine-modified silica aerogels with epoxies: Mechanically strong lightweight porous materials, Chemistry of Materials 17 (2005), pp.1085;

[57] B. N. Nguyen, M. A. B. Meador, M. E. Tousley, B. Shonkwiler, L. McCorkle, D. A. Scheiman, and A.Palczer, Tailoring elastic properties of silica aerogels cross-linked with polystyrene, ACS Applied Materials and Interfaces 1 (2009), pp.621;

[58] U. F. Ilhan, E. F. Fabrizzio, L. McCorkle, D. A. Scheiman,; A. Dass, A. Palczer, M. A. B. Meador, J. C. Johnston, and N. Leventis, Hydrophobic monolithic aerogels by nanocasting polystyrene on amine-modified silica, Journal of Materials Chemistry 16 (2006), pp.3046;

[59] S. Mulik, C. Sotiriou-Leventis, G. Churu, H. Lu, N.Leventis, Cross-linking 3D assemblies of nanoparticles into mechanically strong aerogels by surface-initiated free-radical polymerization, Chemistry of Materials 20(2008), pp.5035;

[60] D.J. Boday, K. A. DeFriend, K. V. Wilson, J. D. Coder, and D. A. Loy, Formation of polycyanoacrylate - Silica nanocomposites by chemical vapor deposition of cyanoacrylates on aerogels, Chemistry of Materials 20 (2008), pp.2847;

[61] K. Finlay, M.D. Gawryla, and D.A. Schiraldi, Biologically based fiber-reinforced/clay aerogel composites, Industrial & Engineering Chemistry Research 47 (2008), pp.615;

[62] http://aerogel.com;

[63] US patents: G.L. Gould, J.K. Lee, C.J. Stepanian, and K.P. Lee, High strength, nanoporous bodies reinforced with fibrous materials, United States Patent Application (2007), 20070222116;

[64] US patents: J. Ryu, Flexible aerogel superinsulation and its manufacture, United States Patent (2000), 6068882.

[65] S. Sequeira, D.V. Evtuguin, I. Portugal, and A.P. Esculcas, Synthesis and characterisation of cellulose/silica hybrids obtained by heteropoly acid catalysed sol-gel process, Materials Science & Engineering C 27 (2007), pp. 172;

[66] S. Sequeira, D.V. Evtuguin, and I. Portugal, Preparation and Properties of Cellulose/Silica Hybrid Composites, Polymer Composites 30(2009), pp.1275;

[67] A. V. Rao, M.M. Kulkarni, D.P. Amalnerkar, and T. Seth, Superhydrophobic silica aerogels based on methyltrimethoxysilane precursor, Journal of Non- Crystalline Solids 330 (2003) 187.

[68] A. V. Rao and S.D. Bhagat, Synthesis and physical properties of TEOS-based silica aerogels prepared by two step (acid-base) sol-gel process, Solid State Sciences 6 (2004), pp.945;

[69] A. V. Rao, G.M. Pajonk, S.D. Bhagat, and P. Barboux, Comparative studies on the surface chemical modification of silica aerogels based on various organosilane compounds of the type RnSiX4-n, Journal of Non- Crystalline Solids 350 (2004),

pp.216;

[70] A. V. Rao, S. D. Bhagat, H. Hiroshima, and G.M. Pajonk, Synthesis of flexible silica aerogels using methyltrimethoxysilane (MTMS) precursor, Journal of Colloid and Interface Science 300 (2006), pp.279;

[71] A. V. Rao, N.D. Hegde, and H. Hirashima, Absorption and desorption of organic liquids in elastic superhydrophobic silica aerogels, Journal of Colloid and Interface Science 305 (2007), pp.124;

[72] D.Y. Nadargi, S. S. Latthe, H. Hirashima, and A. V. Rao, Studies on rheological properties of methyltriethoxysilane (MTES) based flexible superhydrophobic silica aerogels, Microporous and Mesoporous Materials 117 (2009), pp.617;

[73] K. Kanamori, M. Aizawa, K. Nakanishi, and T. Hanada, New transparent methylsilsesquioxane aerogels and xerogels with improved mechanical properties, Advanced Materials 19 (2007), pp.1589;

[74] K. Kanamori, M. Aizawa, K. Nakanishi, and T. Hanada, Elastic organic-inorganic hybrid aerogels and xerogels, Journal of Sol-Gel Science and Technology 48(2008), pp.172;

[75] T. Woignier, J. Phalippou, and R. Vacher in Better Ceramics Through Chemistry III, eds. C.J. Brinker, D.E. Clark, D.R. Ulrich (Materials Research Society, Pittsburgh, 1988), pp.697;

[76] T. Woignier, J. Phalippou, R. Sempere, and J. Pelous, Analysis of the elastic behavior of silica aerogels taken as a percolating system, Journal de Physique 49(1988), pp. 289;

[77] L. J. Gibson, and M. F. Ashby, Cellular solids: Structure and Properties (Cambridge Solid State Science Series, 2nd editon, 1999);

[78] L.W. Hrubesh, R.W. Pekala, Thermal-Properties of organic and inorganic aerogels, Journal of Materials Research 9 (1994), pp.731;

[79] J. Fricke, E. Hummer, H-J. Morper, and P. Scheuerpflug, in Revue de Physique Apliquee, edited by R. Vacher, J. Phalippou, J. Pelous, and T. Woignier (Proc. 2nd Int. Symp. Aerogels 24, C4, Les Editions de Physique, Les Ulis Cedex, 1989), pp.87 ;

[80] X. Lu, M. C. Arduini-Schuster, J. Kuhn, O. Nilsson, J. Fricke, and R.W. Pekala, Thermal-Conductivity of monolithic organic aerogels, Science 255(1992), pp. 974;

[81] M. Kaviany, Principles of Heat Transfer in Porous Media (Springer-Verlag, New

York, 1991), pp.333;

[82] R. Caps and J. Fricke, in Aerogels, Springer Proceedings in Physics, edited by J. Fricke (Springer-Verlag, Heidelberg, Germany, 1986), Vol. 6, pp.110;

[83] http://eetd.lbl.gov/ECS/aerogels/sa-kinetic.html from Microstructured Materials Group at Lawrence Berkeley National Laboratory.

[84] A.A Anappara, S. Rajeshkumar, P. Mukundan, P.R.S. Warrier, S. Ghosh, and K.G.K. Warrier, Impedance spectroscopic studies of sol-gel derived subcritically dried silica aerogels, Acta Materialia 52 (2004), pp.369;

[85] C.S. Ashley, S.T. Reed, C.J. Brinker, R.J. Walco, R.E. Ellefson, J.T. Gill, in: L.L. Hench, J.K. West (Ed&.), Chemical Processing of Advanced Materials (Wiley. New York. 1992) pp.989;

[86] Y. Nagasaka and A. Nagashima, Absolute measurement of the thermal-conductivity of electrically conducting liquids by the transient hot-wire method, Journal of Physics E: Scientific Instruments 14 (1981) pp. 1435;

[87] B.E. Poling, J.M. Prausnitz, J.P. O'Connell, The properties of gases and liquids (McGraw-Hill, New York, 2001), pp.10.42;

[88] L. Vozár, A computer-controlled apparatus for thermal conductivity measurement by the transient hot wire method, Journal of Thermal Analysis 46 (1996), pp. 495;

[89] A.V. Rao, J.M. Pajonk, and D. Haranath, Synthesis of hydrophobic aerogels for transparent window insulation applications, Materials Science and Technology 17 (2001), pp. 343;

[90] T. Woignier, J. Reynes, A. H. Alaoui, I. Beurroies, and J. Phalippou, Different kinds of structure in aerogels: relationships with the mechanical properties, Journal of Non-Crystalline Solids 241 (1998), pp. 45;

[91] N. Leventis, Three-dimensional core-shell superstructures: Mechanically strong aerogels, Accounts of Chemical Research 40(2007), pp.874;

[92] http://www.laponite.com/.